The fold-flip bifurcation

Yu.A. Kuznetsov, H.G.E. Meijer, and L. van Veen*

March 20, 2003

Abstract

The fold-flip bifurcation occurs if a map has a fixed point with multipliers $+1$ and -1 simultaneously. In this paper the normal form of this singularity is calculated explicitly. Both local and global bifurcations of the unfolding are analysed by exploring a close relationship between the derived normal form and the truncated amplitude system for the fold-Hopf bifurcation of ODEs. Two examples are presented, the generalized Hénon map and an extension of the Lorenz-84 model. In the latter example the first, second and third order derivatives of the Poincaré map are computed to find the normal form coefficients.

Running title: The fold-flip bifurcation.

*Mathematical Institute, Utrecht University, PO Box 80.010, 3508 TA Utrecht, The Netherlands

1 Introduction

Consider a family of discrete-time dynamical systems generated by the map

$$x \mapsto F(x, \alpha), \tag{1}$$

where $F : \mathbb{R}^n \times \mathbb{R}^m \to \mathbb{R}^n$ is sufficiently smooth.

It is well known (see, for example, Arnold [1983] for the general theory and Kuznetsov [1998] for the derivation of computational formulas reported below) that in *generic one-parameter* families (1) only the following three bifurcations of fixed points happen:

1. *Fold*: The fixed point has a simple eigenvalue $\lambda_1 = 1$ and no other eigenvalues are on the unit circle. The restriction of (1) to a one-dimensional center manifold at the critical parameter value has the form

$$\xi \mapsto \xi + \frac{1}{2}a\xi^2 + O(\xi^3), \tag{2}$$

where $a \neq 0$. When the parameter crosses the critical value, two fixed points of (1) coalesce and disappear. This bifurcation is often called the *saddle-node bifurcation*. If $Av = F_x v$ and $B(u, v) = F_{xx}[u, v]$ are evaluated at the critical fixed point, then

$$a = \langle q^*, B(q, q)\rangle, \tag{3}$$

where $Aq = q$, $A^T q^* = q^*$, and $\langle q^*, q\rangle = 1$. Here and in what follows $\langle u, v\rangle = \bar{u}^T v$ is the standard scalar product in $\mathbb{C}^n$ (or $\mathbb{R}^n$).

2. *Flip*: The fixed point has a simple eigenvalue $\lambda_1 = -1$ and no other eigenvalues are on the unit circle. The restriction of (1) to a one-dimensional center manifold at the critical parameter value can be transformed to the normal form

$$\xi \mapsto -\xi + \frac{1}{6}b\xi^3 + O(\xi^4), \tag{4}$$

where $b \neq 0$. When the parameter crosses the critical value, a cycle of period 2 bifurcates from the fixed point in (1). This phenomenon is often called the *period-doubling bifurcation*. If $C(u, v, w) = F_{xxx}[u, v, w]$ is evaluated at the critical fixed point, then

$$b = \langle p^*, C(p, p, p) + 3B(p, (I_n - A)^{-1}B(p, p))\rangle, \tag{5}$$

where I_n is the unit $n \times n$ matrix, $Ap = -p$, $A^T p^* = -p^*$, and $\langle p^*, p\rangle = 1$.

3. *Neimark-Sacker*: The fixed point has simple critical eigenvalues $\lambda_{1,2} = e^{\pm i\theta_0}$ and no other eigenvalues are on the unit circle. Assume that

$$e^{iq\theta_0} - 1 \neq 0, \quad q = 1, 2, 3, 4 \quad \text{(no strong resonances)}.$$

Then, the restriction of (1) to a two-dimensional center manifold at the critical parameter value can be transformed to the normal form

$$\eta \mapsto \eta e^{i\theta_0}\left(1 + \frac{1}{2}d|\eta|^2\right) + O(|\eta|^4), \tag{6}$$

where η is a complex variable and d is a complex number. Further assume that

$$c = \text{Re } d \neq 0.$$

Under these assumptions, a unique *closed invariant curve* around the fixed point appears in (1) when the parameter crosses the critical value. One has the following expression for d:

$$d = \frac{1}{2} e^{-i\theta_0} \langle v^*, C(v, v, \bar{v}) + 2B(v, (I_n - A)^{-1} B(v, \bar{v})) + B(\bar{v}, (e^{2i\theta_0} I_n - A)^{-1} B(v, v)) \rangle, \quad (7)$$

where $Av = e^{i\theta_0} v$, $A^T v^* = e^{-i\theta_0} v^*$, and $\langle v^*, v \rangle = 1$.

In *generic two-parameter* families, the above listed codim 1 bifurcations occur when we cross the corresponding *bifurcation curve* (defined by the single condition on the eigenvalues) at a typical point. Moreover, one can choose the eigenvectors so that the normal form coefficients a, b, and c will be smooth functions along these curves[1]. While tracing a bifurcation curve in a generic two-parameter family (1), one may encounter a doubly-degenerate singularity if either (i) extra eigenvalues approach the unit circle, thus changing the dimension of the center manifold; or (ii) one of the nonequalities on the normal form coefficients mentioned above becomes an equality. Therefore, the following eleven doubly degenerate (or codim 2) bifurcation points can be met in generic two-parameter families of maps:

D_1 : $\lambda_1 = 1,\ a = 0$ (cusp);
D_2 : $\lambda_1 = -1,\ b = 0$ (generalized flip);
D_3 : $\lambda_{1,2} = e^{\pm i\theta_0},\ c = 0$ (Chenciner point);
D_4 : $\lambda_1 = \lambda_2 = 1$ (1:1 resonance);
D_5 : $\lambda_1 = \lambda_2 = -1$ (1:2 resonance);
D_6 : $\lambda_{1,2} = e^{\pm i\theta_0},\ \theta_0 = \frac{2\pi}{3}$ (1:3 resonance);
D_7 : $\lambda_{1,2} = e^{\pm i\theta_0},\ \theta_0 = \frac{\pi}{2}$ (1:4 resonance);
D_8 : $\lambda_1 = 1,\ \lambda_2 = -1$;
D_9 : $\lambda_1 = 1,\ \lambda_{2,3} = e^{\pm i\theta_0}$;
D_{10} : $\lambda_1 = -1, \lambda_{2,3} = e^{\pm i\theta_0}$;
D_{11} : $\lambda_{1,2} = e^{\pm i\theta_0},\ \lambda_{3,4} = e^{\pm i\theta_1}$.

The cases D_1–D_7 are well understood and presented in many textbooks (see, for example, Arnold [1983]; Arrowsmith and Place [1990]; Kuznetsov [1998]). Notice that these seven are the only possibilities if the map (1) is a Poincaré map associated with a limit cycle in a three-dimensional autonomous system of ODEs: Then there are just two eigenvalues $\lambda_{1,2}$ of the linearization of the Poincaré map and their product is always positive due to the Liouville formula, i.e., $\lambda_1 \lambda_2 > 0$. That is why cases D_8–D_{11} received much less attention. These cases, however, will appear inevitably in more realistic higher-dimensional models.

This paper is devoted to a detailed analysis of case D_8, that we call the *fold-flip bifurcation*. A connection between the corresponding bifurcation of limit cycles and bifurcations of the truncated amplitude system appearing in the anlysis of the fold-Hopf bifurcation of ODEs was first indicated in Arnold et al. [1994]. For maps, this bifurcation has been specially treated

[1]The coefficient θ_0 also has this property.

by Gheiner [1994]. In the present paper we clarify, correct, and extend that analysis. In Sec. 2, we derive the parameter-dependent normal form for a generic fold-flip bifurcation and give explicit expressions for the critical normal form coefficients in 2- and n-dimensional systems. In Sec. 3 we complete the analysis of local bifurcations of the normal form and study global bifurcations by approximating the map by time-shifts along orbits of an auxiliary planar ODE, present (as completely as possible) bifurcation diagrams of the truncated normal form, including computer-generated phase portraits), and then discuss effects of the truncation. Section 4 is devoted to the normal form analysis of the fold-flip bifurcation in two examples: A generalized Hénon map and the Poincaré map for a 4-dimensional extension of the Lorenz-84 model. The generalized Hénon map appears in the study of bifurcations of diffeomorphisms with codim 2 homoclinic and heteroclinic tangencies, while the second model describes the atmospheric circulation and, to our best knowledge, is the first autonomous ODE system appearing in applications that exhibits the fold-flip bifurcation. For this model, we compute numerically the partial derivatives of the Poincaré map (see Appendix) and then use them to evaluate the critical normal form coefficients and, thus, to demonstrate the nondegeneracy of the fold-flip in this case.

2 Normal Form for the Fold-Flip Bifurcation

2.1 Planar normal form

Proposition 2.1.1 (Critical normal form) *Suppose a smooth map $F_0 : \mathbb{R}^2 \to \mathbb{R}^2$ has the form*

$$\begin{pmatrix} \xi_1 \\ \xi_2 \end{pmatrix} \mapsto \begin{pmatrix} \xi_1 + \sum\limits_{i+j=2,3} \frac{1}{i!j!} g_{ij} \xi_1^i \xi_2^j \\ -\xi_2 + \sum\limits_{i+j=2,3} \frac{1}{i!j!} h_{ij} \xi_1^i \xi_2^j \end{pmatrix} + O(\|\xi\|^4) \tag{8}$$

and $h_{11} \neq 0$. Then F_0 is smoothly equivalent near the origin to the map

$$\begin{pmatrix} x_1 \\ x_2 \end{pmatrix} \mapsto \begin{pmatrix} x_1 + \frac{1}{2}a(0)x_1^2 + \frac{1}{2}b(0)x_2^2 + \frac{1}{6}c(0)x_1^3 + \frac{1}{2}d(0)x_1x_2^2 \\ -x_2 + x_1x_2 \end{pmatrix} + O(\|x\|^4), \tag{9}$$

where

$$a(0) = \frac{g_{20}}{h_{11}}, \quad b(0) = g_{02}h_{11}, \quad c(0) = \frac{1}{h_{11}^2}\left(g_{30} + \frac{3}{2}g_{11}h_{20}\right), \tag{10}$$

$$d(0) = \frac{3g_{02}(h_{02}h_{20} + 2h_{21} - 2g_{11}h_{20}) - g_{20}(3h_{02}^2 + 2h_{03})}{6h_{11}} - g_{11}^2 + g_{12} + \frac{1}{2}g_{11}h_{02} - h_{02}^2 - \frac{2}{3}h_{03}. \tag{11}$$

Proof:

Step 1 (Quadratic terms) Applying to (8) a polynomial coordinate transformation

$$\begin{cases} \xi_1 &= x_1 + \frac{1}{2}G_{20}x_1^2 + G_{11}x_1x_2 + \frac{1}{2}G_{02}x_2^2, \\ \xi_2 &= x_2 + \frac{1}{2}H_{20}x_1^2 + H_{11}x_1x_2 + \frac{1}{2}H_{02}x_2^2, \end{cases} \tag{12}$$

we obtain:

$$\begin{aligned} x_1 &\mapsto x_1 + \frac{1}{2}g_{20}x_1^2 + (g_{11} + 2G_{11})x_1x_2 + \frac{1}{2}g_{02}x_2^2 + \cdots, \\ x_2 &\mapsto -x_2 + \frac{1}{2}(h_{20} - 2H_{20})x_1^2 + h_{11}x_1x_2 + \frac{1}{2}(h_{02} - 2H_{02})x_2^2 + \cdots, \end{aligned}$$

where dots stand for higher-order terms. By setting

$$G_{11} = -\frac{1}{2}g_{11}, \quad H_{20} = \frac{1}{2}h_{20}, \quad H_{02} = \frac{1}{2}h_{02}, \tag{13}$$

we eliminate as many quadratic terms as possible. The remaining quadratic terms are called *resonant*.

Step 2 (Cubic terms) Assume now that Step 1 is already done, so that (8) has only resonant quadratic and all cubic terms. Consider a polynomial transformation:

$$\begin{cases} \xi_1 = & x_1 + \frac{1}{6}G_{30}x_1^3 + \frac{1}{2}G_{21}x_1^2x_2 + \frac{1}{2}G_{12}x_1x_2^2 + \frac{1}{6}G_{03}x_2^3, \\ \xi_2 = & x_2 + \frac{1}{6}H_{30}x_1^3 + \frac{1}{2}H_{21}x_1^2x_2 + \frac{1}{2}H_{12}x_1x_2^2 + \frac{1}{6}H_{03}x_2^3, \end{cases} \tag{14}$$

Obviously, it does not change the quadratic terms. After this transformation, we get

$$x_1 \mapsto x_1 + \frac{1}{2}g_{20}x_1^2 + \frac{1}{2}g_{02}x_2^2 + \frac{1}{6}g_{30}x_1^3 + \frac{1}{2}(g_{21}+2G_{21})x_1^2x_2 + \frac{1}{2}g_{12}x_1x_2^2 + \frac{1}{6}(g_{03}+2G_{03})x_2^3 + \cdots$$

and

$$x_2 \mapsto -x_2 + h_{11}x_1x_2 + \frac{1}{6}(h_{30}-2H_{30})x_1^3 + \frac{1}{2}h_{21}x_1^2x_2 + \frac{1}{2}(h_{12}-2H_{12})x_1x_2^2 + \frac{1}{6}h_{03}x_2^3 + \cdots .$$

By setting

$$G_{21} = -\frac{1}{2}g_{21}, \quad G_{03} = -\frac{1}{2}g_{03}, \quad H_{30} = \frac{1}{2}h_{30}, \quad H_{12} = \frac{1}{2}h_{12},$$

we eliminate four cubic terms. The remaining cubic terms are also called *resonant*. They are not altered by (14).

Step 3 (More cubic terms) The coefficients H_{11}, G_{20}, and G_{02} of (12) do not affect the quadratic terms of (8) but alter its cubic terms. Taking into account (13) while computing the cubic terms of the transformed map, we obtain

$$\begin{aligned} x_1 \;\mapsto\; & x_1 + \frac{1}{2}g_{20}x_1^2 + \frac{1}{2}g_{02}x_2^2 + \frac{1}{6}\left(g_{30} + \frac{3}{2}g_{11}h_{20}\right)x_1^3 \\ & + \frac{1}{2}\left(2g_{02}H_{11} - g_{02}G_{20} + (g_{20}+2h_{11})G_{02} + \frac{1}{2}g_{11}h_{02} + g_{12} - g_{11}^2\right)x_1x_2^2 + \cdots \end{aligned}$$

and

$$\begin{aligned} x_2 \;\mapsto\; & -x_2 + h_{11}x_1x_2 + \frac{1}{2}\left(g_{20}H_{11} + h_{11}G_{20} - g_{11}h_{20} + \frac{1}{2}h_{02}h_{20} + h_{21}\right)x_1^2x_2 \\ & + \frac{1}{6}\left(3g_{02}H_{11} + 3G_{02}h_{11} + h_{03} + \frac{3}{2}h_{02}^2\right)x_2^3 + \cdots , \end{aligned}$$

where only the resonant cubic terms are displayed. Thus, we can try to eliminate three altered terms by selecting H_{11}, G_{20}, and G_{02}. This requires solving the following linear system:

$$\begin{pmatrix} 2g_{02} & -g_{02} & 2h_{11}+g_{20} \\ g_{20} & h_{11} & 0 \\ 3g_{02} & 0 & 3h_{11} \end{pmatrix} \begin{pmatrix} H_{11} \\ G_{20} \\ G_{02} \end{pmatrix} = \begin{pmatrix} -\frac{1}{2}g_{11}h_{02} - g_{12} + g_{11}^2 \\ g_{11}h_{20} - \frac{1}{2}h_{02}h_{20} - h_{21} \\ -h_{03} - \frac{3}{2}h_{02}^2 \end{pmatrix}.$$

Its matrix has zero determinant. However, using the nondegeneracy condition $h_{11} \neq 0$, we can eliminate the resonant cubic terms in the second component of the normal form. Thus, we set

$$H_{11} = 0 \tag{15}$$

and from the above linear system obtain:

$$G_{02} = -\frac{1}{h_{11}}\left(\frac{1}{3}h_{03} + \frac{1}{2}h_{02}^2\right), \quad G_{20} = \frac{1}{h_{11}}\left(g_{11}h_{20} - h_{21} - \frac{1}{2}h_{02}h_{20}\right). \tag{16}$$

Step 4 (Final transformation) Transform now the original map (8) using (12) with the coefficients (13) defined in Step 1, and (15), (16) defined in Step 3. This results in a map with resonant quadratic terms, nonresonant cubic terms, and only two remaining resonant cubic terms in the first component. Transformation (14) from Step 2 allows then to eliminate all nonresonant cubic terms, while keeping unchanged all remaining quadratic and cubic resonant terms. Finally, perform the linear scaling

$$x_1 \mapsto \frac{x_1}{h_{11}}$$

to put the coefficient in front of x_1x_2 in the second component equal to one. This results in the expressions (10) and (11) for the critical normal form coefficients. □

Remark 2.1.2 Gheiner [1994] gave the same critical normal form (9), but here we have derived explicit expressions for the critical normal form coefficients. ▷

Proposition 2.1.3 (Parameter-dependent normal form) *Consider a two-parameter family of planar maps*

$$\xi \mapsto F(\xi, \alpha), \quad \xi \in \mathbb{R}^2, \alpha \in \mathbb{R}^2,$$

where $F : \mathbb{R}^2 \times \mathbb{R}^2 \to \mathbb{R}^2$ *is smooth and such that*

1. $F_0 : \mathbb{R}^2 \to \mathbb{R}^2,\ \xi \mapsto F_0(\xi) = F(\xi, 0)$ *satisfies the assumptions of* Proposition 2.1.1;
2. *The map* $T : \mathbb{R}^2 \times \mathbb{R}^2 \to \mathbb{R}^2 \times \mathbb{R} \times \mathbb{R}$, *defined by*

$$\begin{pmatrix} \xi \\ \alpha \end{pmatrix} \mapsto T(\xi, \alpha) = \begin{pmatrix} F(\xi, \alpha) - \xi \\ \det F_\xi(\xi, \alpha) + 1 \\ \mathrm{Tr}\ F_\xi(\xi, \alpha) \end{pmatrix} \tag{17}$$

is regular at $(\xi, \alpha) = (0, 0)$.

Then F *is smoothly equivalent near the origin to a family*

$$\begin{pmatrix} x_1 \\ x_2 \end{pmatrix} \mapsto \begin{pmatrix} \mu_1 + (1+\mu_2)x_1 + \frac{1}{2}a(\mu)x_1^2 + \frac{1}{2}b(\mu)x_2^2 + \frac{1}{6}c(\mu)x_1^3 + \frac{1}{2}d(\mu)x_1x_2^2 \\ -x_2 + x_1x_2 \end{pmatrix} + O(\|x\|^4), \tag{18}$$

where all coefficients are smooth functions of μ *and their values at* $\mu_1 = \mu_2 = 0$ *are given by* (10) *and* (11).

Remark 2.1.4 Map (17) can be substituted by the map

$$\begin{pmatrix} \xi \\ \alpha \end{pmatrix} \mapsto \begin{pmatrix} F(\xi, \alpha) - \xi \\ \det(F_\xi(\xi, \alpha) + I_2) \\ \det(F_\xi(\xi, \alpha) - I_2) \end{pmatrix}.$$

The regularity of both maps implies the transversality of the map F to the critical manifold in the space of 2-jets. ▷

Proof of Proposition 2.1.3:

Expand F in ξ at $\xi = 0$ for any small $\|\alpha\|$:

$$\xi \mapsto F(\xi, \alpha) = \gamma(\alpha) + A(\alpha)\xi + R(\xi, \alpha),$$

where $\gamma(0) = 0$ and $R(\xi, \alpha) = O(\|\xi\|^2)$. The first assumption implies the existence of two eigenvectors, $q(\alpha)$ and $p(\alpha)$ in $\mathbb{R}^2$, such that

$$A(\alpha)q(\alpha) = \lambda_1(\alpha)q(\alpha), \quad A(\alpha)p(\alpha) = \lambda_2(\alpha)p(\alpha),$$

where $\lambda_1(0) = 1$ and $\lambda_2(0) = -1$. Note that, due to the simplicity of the eigenvalues ± 1 of $A(0)$, $\lambda_{1,2}$ depend smoothly on α, and q, p can also be chosen such that they are smooth functions of α. Any $\xi \in \mathbb{R}^2$ can now be represented for all small $\|\alpha\|$ as

$$\xi = \eta_1 q(\alpha) + \eta_2 p(\alpha),$$

where $\eta = (\eta_1, \eta_2)^T \in \mathbb{R}^2$. One can compute the components of η explicitly:

$$\eta_1 = \langle q^*(\alpha), \xi \rangle, \quad \eta_2 = \langle p^*(\alpha), \xi \rangle,$$

where

$$A^T(\alpha)q^*(\alpha) = \lambda_1(\alpha)q^*(\alpha), \quad A^T(\alpha)p^*(\alpha) = \lambda_2(\alpha)p^*(\alpha)$$

and $\langle q^*(\alpha), q(\alpha) \rangle = \langle p(\alpha)^*, p(\alpha) \rangle = 1$. Since $\langle q^*(\alpha), p(\alpha) \rangle = \langle p^*(\alpha), q(\alpha) \rangle = 0$, the map F, when expressed in the η-coordinates, takes the form

$$\begin{pmatrix} \eta_1 \\ \eta_2 \end{pmatrix} \mapsto \begin{pmatrix} \sigma_1(\alpha) + \lambda_1(\alpha)\eta_1 + S_1(\eta, \alpha) \\ \sigma_2(\alpha) + \lambda_2(\alpha)\eta_2 + S_2(\eta, \alpha) \end{pmatrix}, \tag{19}$$

where

$$\begin{pmatrix} \sigma_1(\alpha) \\ \sigma_2(\alpha) \end{pmatrix} = \begin{pmatrix} \langle q^*(\alpha), \gamma(\alpha) \rangle \\ \langle p^*(\alpha), \gamma(\alpha) \rangle \end{pmatrix}, \quad \begin{pmatrix} S_1(\eta, \alpha) \\ S_2(\eta, \alpha) \end{pmatrix} = \begin{pmatrix} \langle q^*(\alpha), R(\eta_1 q(\alpha) + \eta_2 p(\alpha), \alpha) \rangle \\ \langle p^*(\alpha), R(\eta_1 q(\alpha) + \eta_2 p(\alpha), \alpha) \rangle \end{pmatrix}.$$

Expanding $S_{1,2}(\eta, \alpha)$ further, we can write (19) as

$$\begin{pmatrix} \eta_1 \\ \eta_2 \end{pmatrix} \mapsto \begin{pmatrix} \sigma_1(\alpha) + \lambda_1(\alpha)\eta_1 + \displaystyle\sum_{i+j=2,3} \frac{1}{i!j!} g_{ij}(\alpha)\eta_1^i \eta_2^j \\ \\ \sigma_2(\alpha) + \lambda_2(\alpha)\eta_2 + \displaystyle\sum_{i+j=2,3} \frac{1}{i!j!} h_{ij}(\alpha)\eta_1^i \eta_2^j \end{pmatrix} + O(\|\eta\|^4). \tag{20}$$

Now we want to put (20) in the form (18) by means of a smooth coordinate transformation that depends smoothly on the parameters. Consider the following change of variables:

$$\begin{cases} \eta_1 &= x_1 + \varepsilon_0(\alpha) + \varepsilon_1(\alpha)x_2 + \dfrac{1}{2}G_{20}(\alpha)x_1^2 + G_{11}(\alpha)x_1x_2 + \dfrac{1}{2}G_{02}(\alpha)x_2^2 + \\ & \qquad \dfrac{1}{2}G_{21}(\alpha)x_1^2x_2 + \dfrac{1}{6}G_{03}(\alpha)x_2^3, \\ \eta_2 &= x_2 + \delta_0(\alpha) + \delta_1(\alpha)x_1 + \dfrac{1}{2}H_{20}(\alpha)x_1^2 + \dfrac{1}{2}H_{02}(\alpha)x_2^2 + \\ & \qquad \dfrac{1}{6}H_{30}(\alpha)x_2^3 + \dfrac{1}{2}H_{12}(\alpha)x_1x_2^2, \end{cases} \tag{21}$$

where all coefficients are as yet unknown smooth functions of α such that $\varepsilon_i(0) = \delta_i(0) = 0$ for $i = 0, 1$. Obviously, for $\alpha = 0$ (21) reduces to the transformation introduced in Step 4 of the proof of Proposition 2.1.1 just before the final scaling.

Require now that the Taylor expansion of (20), in the x-coordinates and up to and including cubic terms, takes the form

$$\begin{pmatrix} x_1 \\ x_2 \end{pmatrix} \mapsto \begin{pmatrix} \mu_1(\alpha) + (1+\mu_2(\alpha))x_1 + \frac{1}{2}A(\alpha)x_1^2 + \frac{1}{2}B(\alpha)x_2^2 + \frac{1}{6}C(\alpha)x_1^3 + \frac{1}{2}D(\alpha)x_1x_2^2 \\ -x_2 + E(\alpha)x_1x_2 \end{pmatrix},$$

where, $\mu_1(0) = \mu_2(0) = 0$. After all substitutions, this requirement translates into a system of algebraic equations:

$$Q(\varepsilon_0, \varepsilon_1, \delta_0, \delta_1, \mu_1, \mu_2, G_{20}, G_{11}, G_{02}, G_{21}, G_{03}, H_{20}, H_{02}, H_{30}, H_{12}, A, B, C, D, E) = 0,$$

where $Q : \mathbb{R}^{20} \to \mathbb{R}^{20}$ results from equating the corresponding Taylor coefficients. For the Jacobi matrix $J = DQ$ of this system evaluated at

$$\varepsilon_0 = \varepsilon_1 = \delta_0 = \delta_1 = \mu_1 = \mu_2 = 0$$

we have $\det(J) = -3072h_{11}^3 \neq 0$. Therefore, the Implicit Function Theorem guarantees the local existence and smoothness of the coefficients of the transformation (21) as functions of α.

Moreover, one can show that

$$\begin{cases} \mu_1 &= A_1\alpha_1 + A_2\alpha_2 + O(\|\alpha\|^2), \\ \mu_2 &= \dfrac{1}{h_{11}(0)}\left([(g_{11}(0)B_1 + 2A_3)h_{11}(0) - (h_{02}(0)B_1 + 2B_3)g_{20}]\,\alpha_1 + \right. \\ & \qquad \left. [(g_{11}(0)B_2 + 2A_4)h_{11}(0) - (h_{02}(0)B_2 + 2B_4)g_{20}]\,\alpha_2\right) + O(\|\alpha\|^2), \end{cases} \tag{22}$$

where A_i and B_i are defined by the following expansions of the coefficients of (20):

$$\begin{array}{ll} \sigma_1(\alpha) = A_1\alpha_1 + A_2\alpha_2 + O(\|\alpha\|^2), & \lambda_1(\alpha) = 1 + A_3\alpha_1 + A_4\alpha_2 + O(\|\alpha\|^2), \\ \sigma_2(\alpha) = B_1\alpha_1 + B_2\alpha_2 + O(\|\alpha\|^2), & \lambda_2(\alpha) = -1 + B_3\alpha_1 + B_4\alpha_2 + O(\|\alpha\|^2). \end{array} \tag{23}$$

The functions μ_1 and μ_2 can be taken as the unfolding parameters if the determinant of the Jacobi matrix

$$\Delta = \det\left(\frac{\partial\mu}{\partial(\alpha_1, \alpha_2)}\right)\Big|_{\alpha=0} \neq 0.$$

From (22) we have

$$\Delta = \frac{1}{2h_{11}}\Big[(A_1B_2 - A_2B_1)(g_{11}h_{11} - g_{20}h_{02}) + 2(A_1A_4 - A_2A_3)h_{11} + 2(A_2B_3 - A_1B_4)g_{20}\Big]_{\alpha=0}.$$

On the other hand, taking into account (23), we obtain by direct computations:

$$\det\left(\frac{\partial T}{\partial(\eta, \alpha)}\right)\Big|_{\eta=\alpha=0} = -2\Delta,$$

where T is the map (17) written in the (η, α)-coordinates, i.e., for the map (20). Thus, if $h_{11}(0) \neq 0$, the regularity of (17) at the origin is equivalent to $\Delta \neq 0$.

The scaling

$$x_1 \mapsto \frac{x_1}{E(\mu)}, \quad \mu_1 \mapsto \frac{\mu_1}{E(\mu)},$$

where $E(\mu) = h_{11}(0) + O(\|\alpha\|)$, gives finally (18). Obviously, the critical coefficients are the same as in Proposition 2.1.1. □

2.2 Center Manifold Reduction

We now apply a special version of the center manifold reduction combined with the normalization to our map (see Kuznetsov [1999]; Beyn et al. [2002] and references therein for the case of ordinary differential equations). Consider a two-parameter family of maps $F : \mathbb{R}^n \times \mathbb{R}^2 \to \mathbb{R}^n$,

$$x \mapsto F(x, \alpha), \tag{24}$$

having at $\alpha = 0$ a fixed point $x = 0$ with two simple eigenvalues $\lambda_{1,2} = \pm 1$ and no other critical eigenvalues. We can write:

$$F(x, \alpha) = Ax + A_1\alpha + \frac{1}{2}B(x, x) + B_1(x, \alpha) + \frac{1}{6}C(x, x, x) + \frac{1}{2}C_1(x, x, \alpha) + \cdots ,$$

where only relevant homogeneous linear, quadratic, and cubic terms are displayed. The multilinear forms B and C are defined in Sec. 1, while $B_1(q, \beta) = F_{x\alpha}[q, \beta]$ and $C_1(q, p, \beta) = F_{xx\alpha}[q, p, \beta]$ evaluated at $(x, \alpha) = (0, 0)$. The matrix A has the eigenvalues $\lambda_{1,2} = \pm 1$. Introduce the associated eigenvectors q, q^*, p, p^*, such that

$$\begin{aligned} Aq = q, \quad A^T q^* = q^*, \quad \langle q^*, q\rangle = 1, \\ Ap = -p, \quad A^T p^* = -p^*, \quad \langle p^*, p\rangle = 1. \end{aligned}$$

We want to restrict (24) to its two-dimensional center manifold

$$x = H(w, \beta), \quad H : \mathbb{R}^2 \times \mathbb{R}^2 \to \mathbb{R}^n, \tag{25}$$

depending on two parameters (β_1, β_2). Expand H as

$$H(w, \beta) = \sum_{j_1+j_2+k_1+k_2 \geq 1} \frac{1}{j_1!j_2!k_1!k_2!} h_{j_1 j_2 k_1 k_2} w_1^{j_1} w_2^{j_2} \beta_1^{k_1} \beta_2^{k_2}.$$

Using the freedom of choosing the w-coordinates on the center manifold, we can assume that the restriction of (24) to (25),

$$w \mapsto G(w, \beta), \quad G : \mathbb{R}^2 \times \mathbb{R}^2 \to \mathbb{R}^2, \tag{26}$$

has been put into the form

$$G(w, \beta) = \begin{pmatrix} \beta_1 + (1 + \beta_2)w_1 + \frac{1}{2}a_1(\beta)w_1^2 + \frac{1}{2}b_1(\beta)w_2^2 + \frac{1}{6}c_1(\beta)w_1^3 + \frac{1}{2}c_2(\beta)w_1 w_2^2 \\ -w_2 + e_1(\beta)w_1 w_2 + \frac{1}{2}c_3(\beta)w_1^2 w_2 + \frac{1}{6}c_4(\beta)w_2^3 \end{pmatrix} + O(\|w\|^4)$$

Furthermore, we assume a dependence

$$\alpha = K(\beta) = K_1\beta + O(\|\beta\|^2),$$

where $K : \mathbb{R}^2 \to \mathbb{R}^2$ and K_1 is a 2×2-matrix.

Remark 2.2.1 Note that we have included all cubic terms which become resonant at $\alpha = 0$ in the second component of the normal form (26). In the proof of Proposition 2.1.1 we used primary and secondary normalization. In the primary normalization we applied a quadratic change of coordinates to remove nonresonant quadratic terms, and a cubic change for nonresonant cubic terms. The secondary normalization used quadratic terms to remove some resonant cubic terms, if an additional nondegeneracy condition is satisfied. Sometimes this is called a *hypernormalization*. The coefficient $d(0)$ is changed by this secondary normalization. A priori we do not know if the nondegeneracy condition $h_{11} \neq 0$ is satisfied. Therefore we compute all cubic coefficients in the second component of G, and then use formulas (10) and (11) to obtain the critical coefficients. ▷

The condition of invariance of the center manifold is the homological equation

$$F(H(w,\beta),K(\beta)) = H(G(w,\beta),\beta). \tag{27}$$

Collecting quadratic terms in Eq. (27) we find, for $\beta = 0$,

$$\begin{array}{rcl} (A-I_n)h_{2000} &=& a_1(0)q - B(q,q), \\ (A+I_n)h_{1100} &=& e_1(0)p - B(p,q), \\ (A-I_n)h_{0200} &=& b_1(0)q - B(p,p), \end{array} \tag{28}$$

while the cubic coefficients are obtained from

$$\begin{array}{rcl} (A-I_n)h_{3000} &=& c_1(0)q + 3a_1(0)h_{2000} - 3B(q,h_{2000}) - C(q,q,q), \\ (A-I_n)h_{1200} &=& c_2(0)q + b_1(0)h_{2000} - 2e_1(0)h_{0200} - B(q,h_{0200}) - 2B(p,h_{1100}) - \\ && C(p,p,q), \\ (A+I_n)h_{2100} &=& c_3(0)p + (2e(0) - a(0))\,h_{1100} - 2B(q,h_{1100} - B(p,h_{2000}) - C(q,q,p), \\ (A+I_n)h_{0300} &=& c_4(0)p - 3b_1(0)h_{1100} - 3B(p,h_{0200}) - C(p,p,p). \end{array}$$

Since 1 and -1 are simple eigenvalues of A, the Fredholm solvability condition yields the critical quadratic coefficients

$$a_1(0) = \langle q^*, B(q,q)\rangle,\ e_1(0) = \langle p^*, B(p,q)\rangle,\ b_1(0) = \langle q^*, B(p,p)\rangle,$$

and using the bordering technique described in Kuznetsov [1999] we find

$$\begin{array}{rcl} h_{2000} &=& (A-I)^{INV}\big(\langle q^*, B(q,q)\rangle q - B(q,q)\big), \\ h_{1100} &=& (A+I)^{INV}\big(\langle p^*, B(q,p)\rangle p - B(q,p)\big), \\ h_{0200} &=& (A-I)^{INV}\big(\langle q^*, B(p,p)\rangle q - B(p,p)\big). \end{array}$$

Here $h = L^{INV}R$ denotes the unique solution of the nonsingular *bordered linear system*:

$$\begin{pmatrix} L & v \\ v^* & 0 \end{pmatrix} \begin{pmatrix} h \\ s \end{pmatrix} = \begin{pmatrix} R \\ 0 \end{pmatrix}.$$

It is assumed that L has a one-dimensional null-space, so that $Lv = L^T v^* = 0, \quad \langle v^*, v\rangle = 1$.

It follows from (28) that $\langle q^*, h_{2000}\rangle = \langle q^*, h_{0200}\rangle = \langle p^*, h_{1100}\rangle = 0$. Therefore we can simply write the expressions for the critical cubic coefficients

$$\begin{aligned} c_1(0) &= \langle q^*, C(q,q,q) + 3B(q, h_{2000})\rangle, \\ c_2(0) &= \langle q^*, C(q,p,p) + B(q, h_{0200}) + 2B(p, h_{1100})\rangle, \\ c_3(0) &= \langle p^*, C(q,q,p) + B(p, h_{2000}) + 2B(q, h_{1100})\rangle, \\ c_4(0) &= \langle p^*, C(p,p,p) + 3B(p, h_{0200})\rangle. \end{aligned}$$

Remark 2.2.2 Note that we do calculate $e_1(0)$ in the center manifold reduction. If $e_1(0) \neq 0$, we can scale and, using the previous remark, obtain

$$a(0) = \frac{a_1(0)}{e_1(0)},\ b(0) = b_1(0)e_1(0),\ c(0) = \frac{c_1(0)}{e_1^2(0)},$$

$$d(0) = c_2(0) + \frac{1}{e_1(0)}\left(b_1(0)c_3(0) - \frac{1}{3}(2e_1(0) + a_1(0))c_4(0)\right).$$

Then $a(0), b(0), c(0)$ and $d(0)$ are the coefficients for (9). ▷

For $\beta \neq 0$ we obtain from Eq. (27) the coefficients $h_{j_1j_2k_1k_2}$ and $(K_1)_{ij}$. This tells us how the center manifold and α depend on β in linear approximation. The w-independent terms give

$$(A - I_n)[h_{0010}\ h_{0001}]\beta = \big([q\ 0] - A_1K_1\big)\beta.$$

Here $[h_{0010}\ h_{0001}]$ should be interpreted as a $2 \times n$ matrix and so on. We take the matrix product with q^* and find $q^*A_1K_1 = (1, 0)$. We happen to have some freedom and can scale K_1 and take as a solution

$$K_1 = \frac{1}{\gamma_1^2 + \gamma_2^2}\begin{pmatrix} \gamma_1 & -\gamma_2 \\ \gamma_2 & \gamma_1 \end{pmatrix}, \qquad \text{with } (\gamma_1, \gamma_2) = q^*A_1. \tag{29}$$

Then one can also solve for h_{0010}, h_{0001}. The equations for the other coefficients are

$$\begin{aligned} (A - I_n)[h_{1010}\ h_{1001}] &= [2h_{2000}\ q] - 2[B(q, h_{0010})\ B(q, h_{0001})] - B_1(q, K_1), \\ (A + I_n)[h_{0110}\ h_{0101}] &= [-h_{1100}\ 0] - 2[B(p, h_{0010})\ B(p, h_{0001})] - B_1(p, K_1), \\ (A - I_n)[h_{2010}\ h_{2001}] &= a(0)[h_{1010}\ h_{1001}] + 2[a_1(0)h_{2000}\ h_{2000}] - \\ &\quad 2[B(h_{0010}, h_{2000})\ B(h_{0001}, h_{2000})] - B_1(h_{2000}, K_1) + C_1(q, q, K_1), \\ (A + I_n)[h_{1110}\ h_{1101}] &= e_1(0)[h_{0110}\ h_{0101}] + [e_1(0)h_{1100}\ - h_{1100}] \\ &\quad -2[B(h_{0010}, h_{1100})\ B(h_{0001}, h_{1100})] - B_1(h_{1100}, K_1) - 2C_1(q, p, K_1), \\ (A - I_n)[h_{0210}\ h_{0201}] &= b_1(0)[h_{1010}\ h_{1001}] + 2[b_1(0)h_{2000}\ 0] - \\ &\quad 2[B(h_{0010}, h_{0200})\ B(h_{0001}, h_{0200})] - B_1(h_{0200}, K_1) - C_1(p, p, K_1). \end{aligned}$$

3 Analysis of the Normal Form

Discard the $O(\|x\|^4)$-terms in (18) to obtain the *truncated normal form*:

$$\begin{pmatrix} x_1 \\ x_2 \end{pmatrix} \mapsto N(x,\mu) = \begin{pmatrix} \mu_1 + (1+\mu_2)x_1 + \frac{1}{2}a(\mu)x_1^2 + \frac{1}{2}b(\mu)x_2^2 + \frac{1}{6}c(\mu)x_1^3 + \frac{1}{2}d(\mu)x_1x_2^2 \\ -x_2 + x_1x_2 \end{pmatrix} \quad (30)$$

Remark 3.0.3 Note that (30) is *invariant* under the reflection in the x_1-axis:

$$x \mapsto Rx, \quad R = \begin{pmatrix} 1 & 0 \\ 0 & -1 \end{pmatrix}, \quad (31)$$

for which $R^2 = I_2$. The phase portraits below will reflect this $\mathbb{Z}_2$-symmetry. $\triangleright$

Denote the critical values of the normal form coefficients by

$$a_0 = a(0),\ b_0 = b(0),\ c_0 = c(0),\ d_0 = d(0).$$

In this section, we study local and global bifurcations of the truncated normal form (30), present its bifurcation diagrams, and then briefly discuss relationships between (30) and (9).

3.1 Local codimension 1 bifurcations

Proposition 3.1.1 *The family of maps* (30) *has the following local codimension* 1 *bifurcations in a sufficiently small neighbourhood of* $(x,\mu) = (0,0)$.

1. *There is a curve*

$$t_{fold} : (x_1, x_2, \mu_1) = \left(-\frac{\mu_2}{a_0} + O(\mu_2^2), 0, \frac{\mu_2^2}{2a_0} + O(\mu_2^3) \right),$$

on which a nondegenerate fold bifurcation occurs if $a_0 \neq 0$.

2. *If* $b_0 \neq 0$, *there is a curve* $t_{flip} : (x_1, x_2, \mu_1) = (0,0,0)$ *on which a nondegenerate flip bifurcation occurs.*

3. *If* $b_0 > 0$ *and* $\mu_1 < 0$, *there is a curve*

$$t_{NS} : (x_1, x_2, \mu_2) = \left(0, \sqrt{-\frac{2\mu_1}{b_0}} + O(\mu_1^{3/2}), \frac{(d_0 + 2b_0)\mu_1}{b_0} + O(\mu_1^2) \right),$$

on which a nondegenerate Neimark-Sacker bifurcation of the second iterate of (30) *occurs, provided*

$$a_0^2 b_0 + 3a_0 b_0 + a_0 d_0 - b_0 c_0 \neq 0. \quad (32)$$

Proof: The Jacobi matrix of (30) is

$$A(x,\mu) = N_x(x,\mu) = \begin{pmatrix} 1+\mu_2 + a(\mu)x_1 + \frac{1}{2}c(\mu)x_1^2 + \frac{1}{2}d(\mu)x_2^2 & b(\mu)x_2 + d(\mu)x_1x_2 \\ x_2 & -1+x_1 \end{pmatrix}.$$

Fold bifurcation The map (30) has a fixed point x with multiplier 1 if

$$\begin{cases} N(x,\mu) &= x, \\ \det(A(x,\mu) - I_2) &= 0. \end{cases}$$

Using the Implicit Function Theorem, we see that this algebraic system has a unique solution curve t_{fold} near the origin as described in statement 1. The critical (adjoint) eigenvectors are $q = q^* = (1,0)^T$, while

$$B(p,q) = \begin{pmatrix} a_0p_1q_1 + b_0p_2q_2 + O(\mu_2) \\ p_1q_2 + p_2q_1 \end{pmatrix}.$$

With (3) from Sec. 1, we obtain

$$a_{fold} = a_0 + O(\mu_2),$$

and if $a_0 \neq 0$ we have a nondegenerate (quadratic) fold when $\mu_2 \to 0$.

Flip bifurcation. Another look at the Jacobi matrix above shows that along the curve t_{flip} defined in the statement 2, the truncated normal form (30) has a fixed point with multiplier -1, i.e., this curve satisfies the algebraic system

$$\begin{cases} N(x,\mu) &= x, \\ \det(A(x,\mu) + I_2) &= 0. \end{cases}$$

Now we have $p = p^* = (0,1)^T$ as (adjoint) eigenvector. Clearly $C(p,p,p) = 0$ and we compute the flip coefficient (5) as

$$b_{flip} = \langle p^*, 3B(p,(I_2 - A)^{-1}B(p,p))\rangle = -\frac{3b_0}{\mu_2} + o(1),$$

where $o(1)$ is bounded as $\mu_2 \to 0$. Then, the flip bifurcation is nondegenerate if $b_0 \neq 0$.

Neimark-Sacker bifurcation. Considering the second iterate of (30) we solve for its fixed point with the determinant of the Jacobi matrix equal to one, i.e.,

$$\begin{cases} N(N(x,\mu),\mu) &= x, \\ \det A(N(x,\mu),\mu)\det A(x,\mu) - 1 &= 0. \end{cases}$$

We find the following exact solution to this system:

$$x_1 = 0, \quad b(\mu)x_2^2 + 2\mu_1 = 0, \quad \mu_2 = \frac{d(\mu) + 2b(\mu)}{b(\mu)}\mu_1, \tag{33}$$

which implies the expansion for t_{NS} in the statement 3. Evaluating the Jacobian matrix of the second iterate of (30) on (33), we find

$$A = (N(N(x,\mu),\mu))_x = \begin{pmatrix} 1 + 6\mu_1 + 4\mu_1^2 & 2b(\mu)\sqrt{-\frac{2\mu_1}{b(\mu)}}(1+\mu_1) \\ -2\sqrt{-\frac{2\mu_1}{b(\mu)}}(1+\mu_1) & 1 + 2\mu_1 \end{pmatrix}.$$

For small $\mu_1 < 0$, it has complex eigenvalues $e^{\pm i\theta_0} = 1 + 4\mu_1 + 2\mu_1^2 \pm \sqrt{\mu_1(2+\mu_1)(1+\mu_1)^2}$. Therefore, we find that in the case of $b_0 > 0, \mu_1 < 0$ there is a Neimark-Sacker bifurcation.

We want to know the sign of the first Lyapunov coefficient c_{NS} along (33). We take

$$q = \left(\frac{b(\mu)}{2}\sqrt{-\frac{2\mu_1}{b(\mu)}}\left(1+\sqrt{\frac{2+\mu_1}{\mu_1}}\right),1\right)^T \text{ and } q^* = \left(-\frac{1}{2}\sqrt{-\frac{2\mu_1}{b(\mu)}}\left(1-\sqrt{\frac{2+\mu_1}{\mu_1}}\right),1\right)^T,$$

such that $Aq = e^{i\theta_0}q$ and $A^Tq^* = e^{-i\theta_0}q^*$, with $e^{i\theta_0} = 1 + 4\mu_1 + 2\mu_1^2 - \sqrt{\mu_1(2+\mu_1)(1+\mu_1)^2}$. We should still scale q^*, since $\langle q^*, q\rangle \neq 1$. Next we compute the first Lyapunov coefficient c_{NS} on t_{NS}, using (7) from Sec. 1, where the multilinear forms B and C correspond to the *second iterate* of (30). This gives:

$$c_{NS} = \frac{1}{2}(-a_0^2b_0 - 3a_0b_0 - a_0d_0 + b_0c_0) + o(\mu_1)$$

as $\mu_1 \to 0$. Therefore, the Neimark-Sacker bifurcation of the period-2 cycle of (30) is nondegenerate near the origin, if (32) holds. □

Remark 3.1.2 Gheiner [1994] obtained similar results concerning the fold and flip bifurcations, but some of his calculations are puzzling. The Neimark-Sacker bifurcation was proven to exist, but no attempt was made to analyse it. As we have seen, this bifurcation is nondegenerate under the condition (32) on the critical normal form coefficients. Choosing, as a numerical example, $b = c = d = 1$ we find $a \neq -2 \pm \sqrt{5}$ as the condition for c_{NS} to be nonzero.

3.2 Global bifurcations

As we shall see, the map (30) has two saddle fixed points, which can posses a heteroclinic structure. To study this global bifurcation phenomenon, we derive a vector field, such that the unit shift along its orbits approximates (30). Bifurcations of this vector field are easy to analyse, since it is similar to an amplitude system for the fold-Hopf bifurcation (see Chow et al. [1994]; Kuznetsov [1998]).

Proposition 3.2.1 (Approximating vector field) *In a small neighbourhood of* $(x, \mu) = (0, 0)$*, the truncated normal form* (30) *satisfies*

$$R\,N(x,\mu) = \varphi^1(x,\mu) + O(\|\mu\|^2) + O(\|x\|^2\|\mu\|) + O(\|x\|^4). \tag{34}$$

Here R *is the matrix defined by* (31)*,* φ^t *is the flow generated by the system*

$$\dot{x} = X(x,\mu), \quad x \in \mathbb{R}^2,\ \nu \in \mathbb{R}^2,$$

where the vector field X *is given by*

$$X(x,\mu) = \begin{pmatrix} \mu_1 + \left(-\frac{1}{2}a_0\mu_1 + \mu_2\right)x_1 + \frac{1}{2}a_0x_1^2 + \frac{1}{2}b_0x_2^2 + d_1x_1^3 + d_2x_1x_2^2 \\ \frac{1}{2}\mu_1x_2 - x_1x_2 + d_3x_1x_2^2 + d_4x_2^3 \end{pmatrix}, \tag{35}$$

with

$$d_1 = \frac{1}{6}\left(c_0 - \frac{3}{2}a_0^2\right),\ d_2 = \frac{1}{2}\left(d_0 + \frac{1}{2}b_0(2-a_0)\right),\ d_3 = \frac{1}{4}(a_0-2),\ d_4 = \frac{1}{4}b_0.$$

Proof:

We construct φ^t as the first two components of the flow

$$\xi \mapsto \phi^t(\xi) = \begin{pmatrix} \varphi^t(x,\mu) \\ \mu \end{pmatrix},\quad \xi = \begin{pmatrix} x \\ \mu \end{pmatrix} \in \mathbb{R}^4,$$

generated by a 4-dimensional system with the parameters considered as constant variables:

$$\dot{\xi} = Y(\xi). \tag{36}$$

Here

$$Y(\xi) = J\xi + Y_2(\xi) + Y_3(\xi) + \cdots,\quad J = \begin{pmatrix} 0 & 0 & 1 & 0 \\ 0 & 0 & 0 & 0 \\ 0 & 0 & 0 & 0 \\ 0 & 0 & 0 & 0 \end{pmatrix},\quad Y_k(\xi) = \begin{pmatrix} X_k(\xi) \\ 0 \end{pmatrix},$$

where each X_k is an order-k homogeneous function from $\mathbb{R}^4$ to $\mathbb{R}^2$ with unknown coefficients. Define

$$M(\xi) = \begin{pmatrix} N(x,\mu) \\ \mu \end{pmatrix}$$

and introduce the 4×4 block-diagonal matrix

$$S = \begin{pmatrix} R & 0 \\ 0 & I_2 \end{pmatrix},$$

where R is given in (31). Following Takens [1974], we look for a vector field Y such that $S\,M(\xi) = \phi^1(\xi) + O(\|\xi\|^4)$.

To find the vector field Y explicitly, perform three Picard iterations for (36) as described in Kuznetsov [1998], Chapter 9. We start with setting $\phi_1^t(\xi) = e^{Jt}\xi$. Then, clearly, the linear part of $S\,M(\xi)$ coincides with $\phi_1^1(\xi)$.

Since we know how the result ϕ_2^t of the second Picard iteration should look, we set some coefficients of Y_2 equal to zero immediately:

$$Y_2 = \begin{pmatrix} A_{10}\mu_1 x_1 + A_{01}\mu_2 x_1 + \frac{1}{2}A_{20}x_1^2 + \frac{1}{2}A_{02}x_2^2 \\ B_{11}x_1x_2 + B_{10}\mu_1 x_2 \\ 0 \\ 0 \end{pmatrix}.$$

Then

$$\begin{aligned}\phi_2^t(\xi) &= e^{Jt}\xi + \int_0^t e^{J(t-\tau)} Y_2(\phi_1^\tau(\xi))d\tau \\ &= \begin{pmatrix} x_1 + t\mu_1 \\ x_2 \\ \mu_1 \\ \mu_2 \end{pmatrix} + \begin{pmatrix} (A_{10} + \frac{1}{2}A_{20}t^2)\mu_1 x_1 + A_{01}\mu_2 x_1 + \frac{1}{2}A_{20}x_1^2 + \frac{1}{2}A_{20}x_2^2 \\ B_{11}x_1x_2 + \left(\frac{1}{2}B_{11}t^2 + B_{10}\right)\mu_1 x_2 \\ 0 \\ 0 \end{pmatrix} + O(\|\mu\|^2).\end{aligned}$$

Comparing quadratic terms in $S\ M(\xi)$ and $\phi_2^1(\xi)$, we find the coefficients of Y_2

$$A_{10} = -\frac{1}{2}a_0,\ A_{20} = a_0,\ A_{01} = 1,\ A_{02} = b_0,\ B_{10} = \frac{1}{2},\ B_{11} = -1.$$

Passing on to the cubic part we remark that we are only interested in cubic terms in x. Therefore, we put

$$Y_3 = \begin{pmatrix} \sum_{i+j=3} \frac{1}{i!j!} A_{ij} x_1^i x_2^j \\ \sum_{i+j=3} \frac{1}{i!j!} B_{ij} x_1^i x_2^j \\ 0 \\ 0 \end{pmatrix}$$

and get

$$\begin{aligned}\phi_3^t(\xi) &= e^{Jt}\xi + \int_0^t e^{J(t-\tau)} \left[Y_2(\phi_2^\tau(\xi)) + Y_3(\phi_2^\tau(\xi))\right] d\tau \\ &= \begin{pmatrix} x_1 + t\mu_1 + \frac{1}{2}a_0(t^2-1)x_1\mu_1 + x_1\mu_2 + \frac{1}{2}a_0x_1^2 + \frac{1}{2}b_0x_2^2 \\ x_2 - x_1x_2 + \frac{1}{2}(1-t^2)\mu_1 x_2 \\ \mu_1 \\ \mu_2 \end{pmatrix} + \\ &\begin{pmatrix} \left(\frac{1}{6}A_{30}t + \frac{1}{4}A_{20}^2t^2\right)x_1^3 + tA_{21}x_1^2x_2 + \left(\frac{1}{2}A_{12}t + \frac{1}{4}t^2A_{02}(A_{20}+2B_{11})\right)x_1x_2^2 + \frac{1}{6}tA_{03}x_2^3 \\ \frac{1}{6}tB_{30}x_1^3 + \left(\frac{1}{2}tB_{21} + \frac{1}{4}t^2B_{11}(2B_{11}+A_{20})\right)x_1^2x_2 + tB_{12}x_1x_2^2 + \left(\frac{1}{6}tB_{03} - \frac{1}{4}t^2A_{02}B_{11}\right)x_2^3 \\ 0 \\ 0 \end{pmatrix} \\ &+ O(\|\mu\|^2) + O(\|x\|^2\|\mu\|).\end{aligned}$$

Comparing cubic terms in $S\ M(\xi)$ and $\phi_3^t(\xi)$, we find the coefficients of Y_3:

$$A_{30} = c_0 - \frac{3}{2}a_0^2,\ A_{21} = 0,\ A_{12} = d_0 + \frac{1}{2}b_0(2-a_0),\ A_{03} = 0,$$

$$B_{30} = 0,\ B_{21} = \frac{1}{2}(a_0 - 2),\ B_{12} = 0,\ B_{03} = \frac{3}{2}b_0.$$

This gives the vector field (35) from the Proposition. □

To explore relationships between the map (30) and the vector field (35), consider first local bifurcations of the vector field X. One can check that there are two curves, $t_{fold} : (x_1, x_2, \mu_1) = (-\mu_2/a_0 + O(\mu_2^2), 0, \mu_2^2/(2a_0) + O(\mu_2^3))$ and $t_{flip} : (x_1, x_2, \mu_1) = (0, 0, 0)$, on which equilibria of (35) have a zero eigenvalue. These are the same expansions as we computed for the map (30). The center manifold reduction shows that a fold (saddle-node) bifurcation occurs on the first curve, while a pitchfork bifurcation happens on the second. Next we computed a Hopf bifurcation curve for (35). We get indeed the same expression

$$t_{NS} : (x_1, x_2, \mu_2) = \left(0, \sqrt{-\frac{2\mu_1}{b_0}} + O(\mu_1^{3/2}), \frac{(2b_0 + d_0)\mu_1}{b_0} + O(\mu_1^2)\right)$$

as in Proposition 3.1.1.

Next we can classify the critical phase portraits of the vector field (35). In the usual polar coordinates the vector field at $\mu = 0$ becomes

$$\begin{pmatrix} \dot{r} \\ \dot{\theta} \end{pmatrix} = \begin{pmatrix} r^2\left(\frac{1}{2}a_0\cos^2\theta + (\frac{1}{2}b_0 - 1)\sin^2\theta\right) + O(r^3) \\ -r\sin\theta\left((1 + \frac{1}{2}a_0)\cos^2\theta + \frac{1}{2}b_0\sin^2\theta\right) + O(r^2) \end{pmatrix}.$$

We see that there are invariant lines in the critical normal form if $\dot{\theta} = 0$. This equation is satisfied if $\theta = 0, \pi$, which is expected due to the invariance of the vector field under the map (31). Another possibility is that

$$\tan^2\theta = -\frac{2 + a_0}{b_0}.$$

Therefore, we find six different critical portraits, see Figs. 1 and 2.

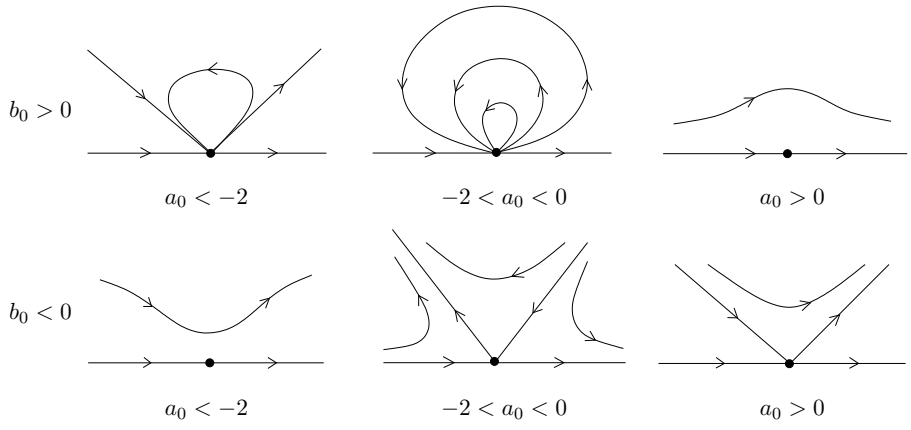

Figure 1: Phase portraits of the approximating vector field X at $\mu = 0$.

The invariant curves born from the Neimark-Sacker bifurcation cannot exist everywhere. They should disappear through global bifurcations. To study these phenomena, we investigate what happens to the cycles of the approximating vector field X born at the Hopf bifurcation.

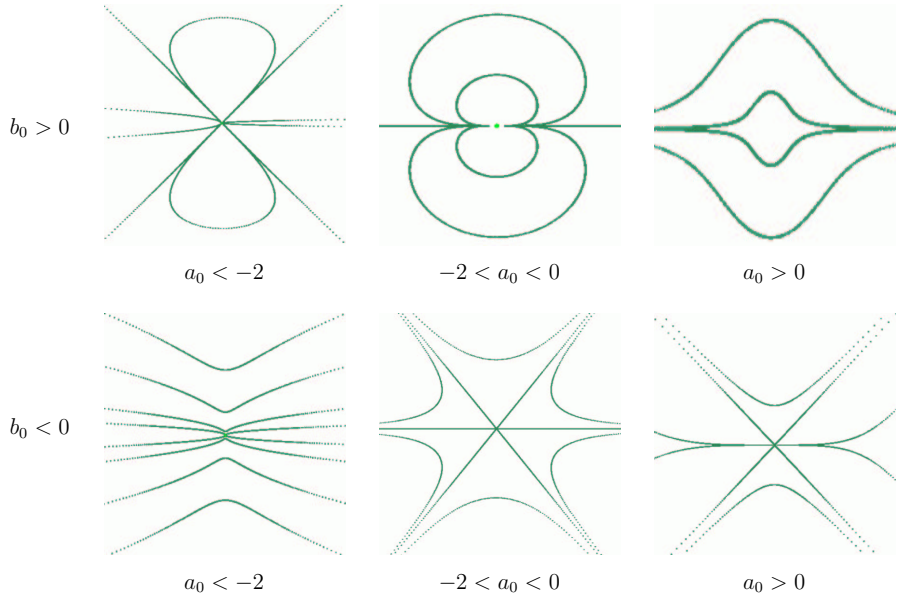

Figure 2: Phase portraits of the normal form N at $\mu = 0$. Compare with the orbits of the vector field to see how the orbits jump.

Proposition 3.2.2 *If $a_0, b_0 > 0$ and $\mu_1 < 0$ then the vector field (35) has two saddles, which are always connected by a heteroclinic orbit along the x_1-axis. There exists another heteroclinic orbit for*

$$t_J : \mu_2 = \frac{\mu_1}{3 + a_0}\left((a_0 + 2)\frac{d_0 + 2b_0}{b} + \frac{c_0 - a_0 - a_0^2}{a_0}\right) + o(\mu_1). \tag{37}$$

Proof:

We first shift the x_1-coordinate in (35) with the transformation

$$x_1 \to x_1 - \left(\frac{\mu_1}{2} + \frac{\mu_2}{a_0}\right).$$

Then we apply a singular rescaling

$$x_1 \to \delta x_1,\ x_2 \to \delta x_2,\ dt \to \frac{x_2^q}{\delta} dt$$

to obtain

$$\left\{\begin{array}{rcl} \dot{x}_1 &=& x_2^q\left(\beta_1 + \frac{1}{2}a_0 x_1^2 + \frac{1}{2}b_0 x_2^2 + \delta[d_1 x_1^3 + d_2 x_1 x_2^2]\right) \\ \dot{x}_2 &=& x_2^q\left(-x_1 x_2 + \delta[\beta_2 x_2 + d_3 x_1^2 x_2 + d_4 x_2^3]\right), \end{array}\right. \tag{38}$$

where

$$\beta_1 = \mu_1 + O(\|\mu\|^2), \quad \beta_2 = \frac{\mu_2}{a_0} + O(\|\mu\|^2).$$

The system (38) can be rewritten as

$$\dot{x} = f(x,\beta) + \delta g(x,\beta) \tag{39}$$

with

$$f(x,\beta) = x_2^q \begin{pmatrix} \beta_1 + \frac{1}{2}a_0 x_1^2 + \frac{1}{2}b_0 x_2^2 \\ -x_1 x_2 \end{pmatrix}, \quad g(x,\beta) = x_2^q \begin{pmatrix} d_1 x_1^3 + d_2 x_1 x_2^2 \\ \beta_2 x_2 + d_3 x_1^2 x_2 + d_4 x_2^3 \end{pmatrix}.$$

For $\delta = 0$ and $q+1 = a_0$, system (39) is Hamiltonian with

$$H(x) = x_2^{q+1}\left(\frac{\beta_1 + \frac{1}{2}a_0 x_1^2}{q+1} + \frac{b_0 x_2^2}{2(q+3)}\right). \tag{40}$$

We have $a_0, b_0 \neq 0$ as nondegeneracy conditions, therefore $q \neq -1$. Level curves of H for several values of a_0 are shown in Fig. 3. Now we treat the term δg in (39) as a small perturbation of the Hamilton system. We should therefore evaluate the Pontryagin-Melnikov function (see Guckenheimer and Holmes [1983, 2002])

$$\Delta(h,\beta) = \oint_{\Gamma_h} f(x_h(\tau),\beta) \wedge g(x_h(\tau),\beta)\, d\tau,$$

where $x_h(\tau)$ is a periodic solution of the Hamiltonian system corresponding to a closed regular level set $\Gamma_h = \{x : H(x) = h\}$, while for $a_0 > 0$

$$\Delta(0,\beta) = \int_{-\infty}^{+\infty} f(x_0(\tau),\beta) \wedge g(x_0(\tau),\beta)\, d\tau,$$

where $x_0(\tau)$ is the nontrivial heteroclinic solution in the critical level set $H = 0$. Notice that $\lim_{h\to 0^-} \Delta(h,\beta) = \Delta(0,\beta)$, since the integral over the trivial heteroclinic connection equals zero. Then $\Delta(0,\beta) = 0$ defines a linear approximation to a curve on which the heteroclinic connection "survives" in (39) for small $\delta \neq 0$. Our computation is analogous to the one in Chow et al. [1994].

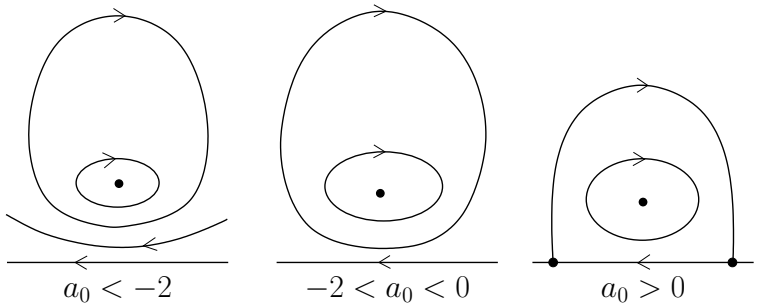

Figure 3: Level curves of H for several a_0

Using Green's formula, we have

$$\begin{aligned}\Delta &= \oint_{\Gamma_h} x_2^q(d_1x_1^3 + d_2x_1x_2^2)dx_2 - x_2^q(\beta_2x_2 + d_3x_1^2x_2 + d_4x_2^3)dx_1 \\ &= \oint_{\Gamma_h} x_2^q\left(d_1x_1^3 + d_2x_1x_2^2 + (q+1)\left(\beta_2x_1 + \frac{1}{3}d_3x_1^3\right) + (q+3)d_4x_1x_2^2\right)dx_2.\end{aligned}$$

Now we use that along Γ_h we have $dH = x_2^q\left(\beta_1 + \frac{1}{2}a_0x_1^2 + \frac{1}{2}b_0x_2^2\right)dx_2 + x_2^{q+1}x_1dx_1 = 0$ and continue

$$\begin{aligned}\Delta &= \oint_{\Gamma_h} x_2^q\left(a_0\beta_2x_1 + \left(d_1 + \frac{1}{3}a_0d_3\right)x_1^3 + (d_2 + (a_0+2)d_4)x_1x_2^2\right)dx_2 \\ &= \oint_{\Gamma_h} x_2^q\left(x_1\left(a_0\beta_2 - \frac{2}{b_0}\beta_1(d_2 + (a_0+2)d_4)\right) + x_1^3\left(d_1 + \frac{1}{3}a_0d_3 - \frac{a_0}{b_0}(d_2 + (a_0+2)d_4)\right)\right)dx_2 \\ &\quad - \oint_{\Gamma_h} \frac{2}{b_0}(d_2 + (a_0+2)d_4)x_1^2x_2^{q+1}dx_1 \\ &= I_{1,h}\left(a_0\beta_2 - \frac{2}{b_0}\beta_1(d_2 + (a_0+2)d_4)\right) + I_{3,h}\left(d_1 + \frac{a_0}{3}d_3 - \frac{a_0}{3b_0}(d_2 + (a_0+2)d_4)\right).\end{aligned}$$

Here we defined $I_{i,h} = \oint_{\Gamma_h} x_2^q x_1^i dx_2$ for $i = 1, 3$.

For $h = 0$ we can evaluate the Pontryagin-Melnikov function as follows. We rewrite our Hamiltonian system as

$$\begin{cases} \dot{x}_1 &= x_2^q\left(\beta_1 + \frac{1}{2}a_0x_1^2 + \frac{1}{2}b_0x_2^2\right) = \frac{b_0}{a_0+2}x_2^{q+2} \\ \dot{x}_2 &= x_2^q(-x_1x_2). \end{cases}$$

Here we used that we are on the zero-level set of the Hamiltonian. The initial conditions are

$$x_1(0) = 0,\ x_2(0) = \sqrt{\frac{-2(a_0+2)\beta_1}{a_0b_0}},$$

which are not changed if we reparametrize $d\tau = x_2^{-q}dt$. We get the new system

$$\begin{cases} \dot{x}_1 &= \frac{b_0}{a_0+2}x_2^2 \\ \dot{x}_2 &= -x_1x_2, \end{cases}$$

which we can explicitly solve with $x_1(\tau) = \gamma\tanh(\gamma\tau),\ x_2(\tau) = x_2(0)\cosh^{-1}(\gamma\tau)$, where

$$\gamma = \sqrt{\frac{-2\beta_1}{a_0}}.$$

Having these solutions, we evaluate $I_{i,0}$ defined above:

$$\begin{aligned} I_{i,0} &= \int_{\Gamma_0} x_2^q x_1^i dx_2 \\ &= -\int_{-\infty}^{\infty} x_2^{a_0} x_1^{i+1} d\tau \\ &= -\int_{-\infty}^{\infty} \frac{\sinh(\gamma\tau)^{i+1}}{\cosh(\gamma\tau)^{i+a_0+1}} d\tau \\ &= -\gamma^i x_2^2(0)(1+(-1)^{i+1}) \frac{\Gamma(\frac{a_0}{2})\Gamma(\frac{2+i}{2})}{2\Gamma(\frac{1}{2}(2+a_0+i))} \end{aligned}$$

In this time-parametrization we used the explicit forms of $x_1(\tau)$ and $x_2(\tau)$. If we now compute the ratio $Q = I_{3,0}/I_{1,0}$, we find

$$Q = \frac{-6\beta_1}{a_0(3+a_0)}.$$

Using the expressions for β_k and d_i, we find that the Melnikov function $\Delta(0,\beta)$ has a zero if

$$\mu_2 = \frac{\mu_1}{3+a_0}\left((a_0+2)\frac{d_0+2b_0}{b_0} + \frac{c_0-a_0-a_0^2}{a_0}\right) + o(\mu_1). \tag{41}$$

This value of μ_2 asymptotically corresponds to the existence of a nontrivial heteroclinic orbit for the perturbed system (38). □

Remark 3.2.3 Taking $a = b = c = d = 1$ we find $\mu_2 = 2\mu_1$. This value was used numerically as well in case (1) of the bifurcation diagrams with DSTOOLS (Back et al. [1992]).

Remark 3.2.4 We derived the linear approximations to both the Neimark-Sacker bifurcation curve, see Proposition 3.1.1,

$$\mu_2 = \frac{d_0+2b_0}{b_0}\mu_1 \tag{42}$$

and the heteroclinic bifurcation curve, see (41). To analyse their relative position, we compute the difference between their slopes:

$$\frac{1}{a_0 b_0(a_0+3)}\left(-a_0 d_0 - 3a_0 b_0 - b_0 a_0^2 + b_0 c_0\right).$$

This shows that the curves coincide in the linear approximation if and only if the Lyapunov coefficient c_{NS} vanishes. Thus, changing the relative position of the two curves changes the stability of the closed invariant curve that appears.

Remark 3.2.5 Moreover, for the vector field we have the uniqueness of the limit cycle. This can be verified as follows. We should evaluate the Pontryagin function on a level curve of the Hamiltonian with $h \neq 0$. Now $Q(h) = I_{1,h}/I_{3,h}$ cannot be evaluated explicitly, but one can prove the monotonicity of Q following Chow et al. [1994]. This implies the uniqueness of the limit cycle. We include some pictures, where we computed $Q(h)$ numerically, to illustrate the monotonicity (see Fig. 4).

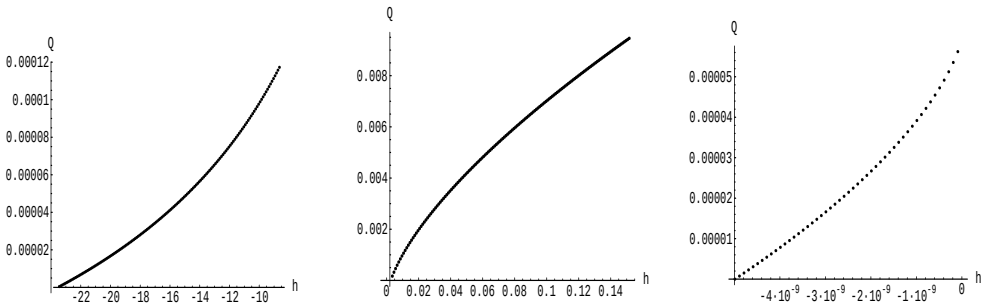

$a_0 = -3$ $a_0 = -\frac{1}{2}$ $a_0 = 2$

Figure 4: Ratio $Q(h) = I_{1,h}/I_{3,h}$

3.3 Bifurcation Diagrams

Although we had six cases for F_0, only four bifurcation diagrams will be reported in Figs. 7–14, because two others differ only at the critical parameter values. We start with the bifurcation diagrams of the vector field (35), which are similar to the bifurcation diagrams of the truncated amplitude system for the fold-Hopf bifurcation (see Guckenheimer and Holmes [1983, 2002], Kuznetsov [1998]). In our study, however, we have to take into account that the Neimark-Sacker bifurcation can be either sub- or super-critical, depending on the sign of c_{NS}. We included these sketches to indicate the direction of the orbit in the phase portraits for the map. The orbits of the map continuously jump from the lower to the upper half plane and back. This is easily understood from (34), which implies that (9) can be approximated by the composition of the unit shift along the orbits of X with the reflection R. We go around the origin in the parameter plane and discuss the phase portraits of the truncated normal form (30). The fold and flip bifurcation curves are denoted by $F_\pm$ and $P_\pm$, respectively. The sub/super-critical Neimark-Sacker bifurcation curve is indicated by $NS_\pm$. For the vector field, J is the heteroclinic bifurcation curve.

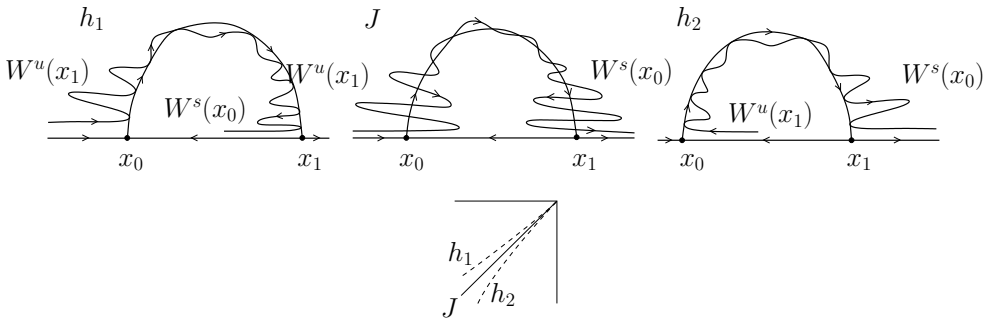

Figure 5: Heteroclinic tangencies appearing in the lines $h_{1,2}$ together with a transversal heteroclinic structure between them.

Remark 3.3.1 We took $c = d = 1$ to generate the pictures related to the map, unless stated otherwise. We use a version of DSTools (Back et al. [1992]), incorporating the algorithms from Krauskopf and Osinga [1998a], Krauskopf and Osinga [1998b]. The colors should be interpreted as follow: Orbits are green, while unstable manifolds of saddles are red and stable manifolds are blue. Note that, with the above choice of the coefficients, c_{NS} is negative in case 1 and positive in case 2. ▷

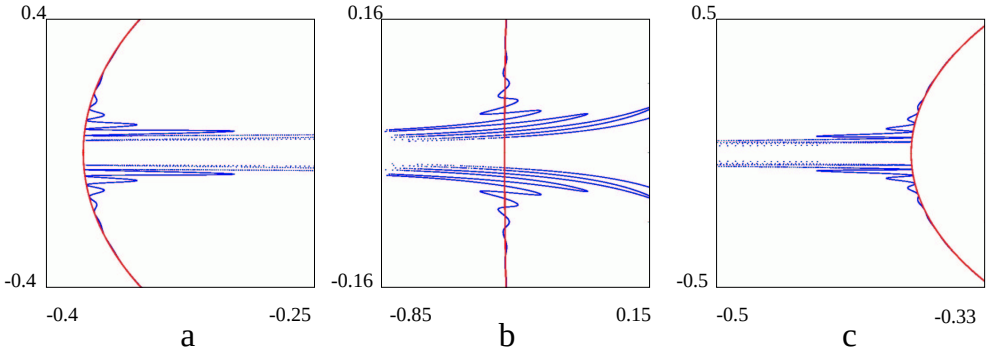

Figure 6: Heteroclinic structures in (30) near the left fixed point for $a = b = d = 1, c = 0.5, \mu_1 = -0.2$ and $\mu_2 = -0.35345880$ (a); $\mu_2 = -0.35347$ (b); $\mu_2 = -0.35349058$ (c).

- **Case 1:** In region **1** orbits merely jump to the right. Crossing F_+ implies the appearance of two fixed points on the horizontal axis. In **2** one of these fixed points is totally unstable, while the other is a saddle. While crossing curve P_+ from **2** to **3**, the unstable fixed point becomes a saddle and an unstable period-2 cycle appears. If $c_{NS} > 0$, an unstable invariant curve "around" the period-2 cycles appears via the Neimark-Sacker bifurcation on NS_+, when we go from **3** to **4+**. The invariant curve disappears through a series of bifurcations associated with the heteroclinic bifurcations near J_+, if we come to **5**. The presence of the J-curve for the vector field implies for the map the existence of two curves, along which homoclinic tangencies occur (see sketches in Fig. 5). Between these two curves, a heteroclinic structure is present. Figure 6 shows invariant curve configurations computed with DSTools. If $c_{NS} < 0$, a stable closed invariant curve emerges in **4-** through a series of bifurcations associated with the heteroclinic structure. This stable invariant curve exists until we cross NS_-, where the stable period-2 cycle becomes attracting in **5**. Next we cross P_- and the period two orbit disappears, leaving us with a stable fixed point and a saddle in **6**. These two collide if we return back to **1**.

- **Case 2:** Fix a phase domain near the origin. Now we start with the two fixed points, one stable and one unstable on the axis in region **1**. Then, crossing the flip curve P_+ to **2**, one fixed point exhibits a period doubling and a period two cycle appears. The fixed points on the horizontal axis collide at the curve F_+ which separates region **2** from region **3**, where a stable period two cycle exists. If $c_{NS} > 0$, then an unstable invariant curve appears when we cross the Neimark-Sacker bifurcation curve NS_+. This invariant

curve grows, until it blows up and disappears from the selected fixed phase domain at some curve B_+. Actually, the invariant curve can lose its smoothness and disappear before touching the boundary of the domain. If $c_{NS} < 0$, then we first encounter the "boundary bifurcation" curve B_-, where a big stable invariant curve appears in our fixed phase domain. The transition from **4-** to **5** destroys the curve via the Neimark-Sacker bifurcation . Finally, crossing of the fold curve F_- produces two fixed points in **6** and through the flip bifurcation on P_- the period-two cycle disappears again as we go back to **1**.

- **Case 3:** We start with a period-two saddle cycle in **1**. Entering **2** through the fold curve F_+ creates two fixed points on the horizontal axis, a saddle and a repelling one. Then, while crossing the flip curve P_+ to **3**, the period two cycle is destroyed and we get two saddles on the x_1-axis. Passing P_- one saddle becomes stable and a period two orbit in **4** is created. Finally, the fixed points on the horizontal axis collide on F_- and we are in region **1** again.

- Case 4. Starting in region **1** we have, as in case 3, a period-two saddle cycle, but also a stable and an unstable fixed point on the x_1-axis. The unstable one becomes a saddle when we enter **2** through the P_+ curve. Then nothing special appears except for a "saddle-like flow" in region **3**, after the saddle and the stable point collided on F_+. Going from **3** to **4** we get a saddle and an unstable point through the fold bifurcation on the curve F_-. We are back in **1**, when the flip bifurcation creates the period-two cycle on P_-.

The diagrams give a rather detailed description of the bifurcations of the truncated normal form (30). However, this description remains incomplete due to the presence of closed invariant curves and heteroclinic tangencies. Indeed, the rotation number on the closed invariant curve can change infinitely many times from rational to irrational and, moreover, the invariant curve can lose smoothness and disappear. Near a heteroclinic tangency, infinite series of bifurcations happen, including cascades of flips and folds (see Gavrilov and Shil'nikov [1972], Gavrilov and Shil'nikov [1973], Gonchenko et al. [1996]).

3.4 Effect of higher order terms

Adding higher order terms to the truncated normal form (30), i.e., restoring (9), complicates the bifurcation picture further.

Using the Implicit Function Theorem, one can prove that for $\|\mu\|$ sufficiently small, the map (9) has the same bifurcations of fixed points and period-2 cycles as (30). More precisely, Proposition 3.1.1 is valid also for the full normal form (9) with *arbitrary* higher order terms. Therefore, we know what to expect locally. In particular, in cases 1 and 2 closed invariant curves appear. Moreover, the unit shift along the orbits of the vector field (35) composed with the reflection approximates (9) as good as (30). This implies that (9) also has two bifurcation curves along which heteroclinic tangencies occur. Between these curves, a heteroclinic structure is present. Higher order terms in (9) do affect these curves, but they both remain tangent to the curve (37) from Proposition 3.2.2.

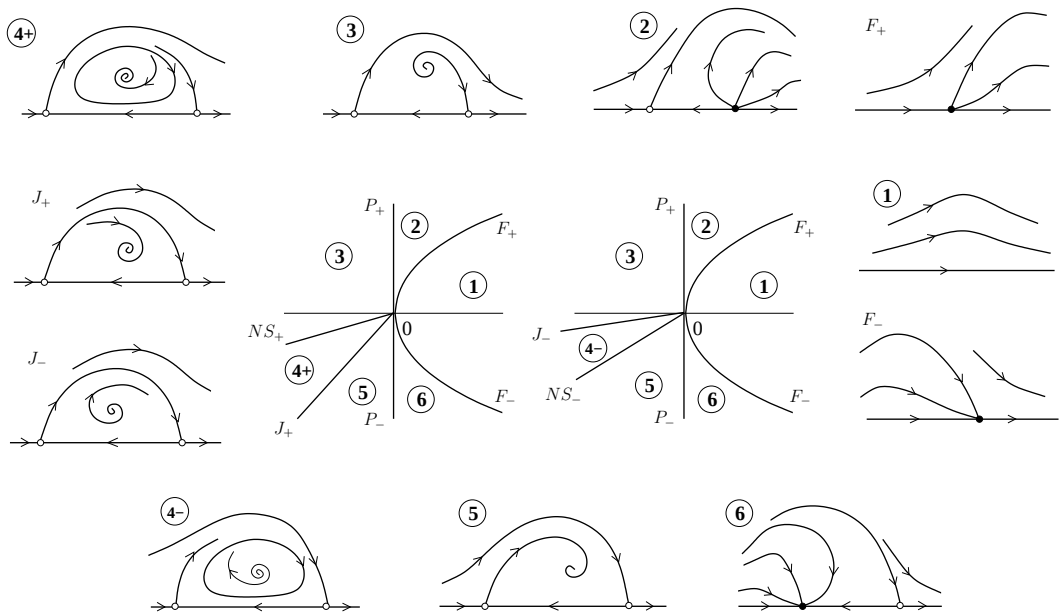

Figure 7: Vector field : Case 1. $a_0 > 0, b_0 > 0$

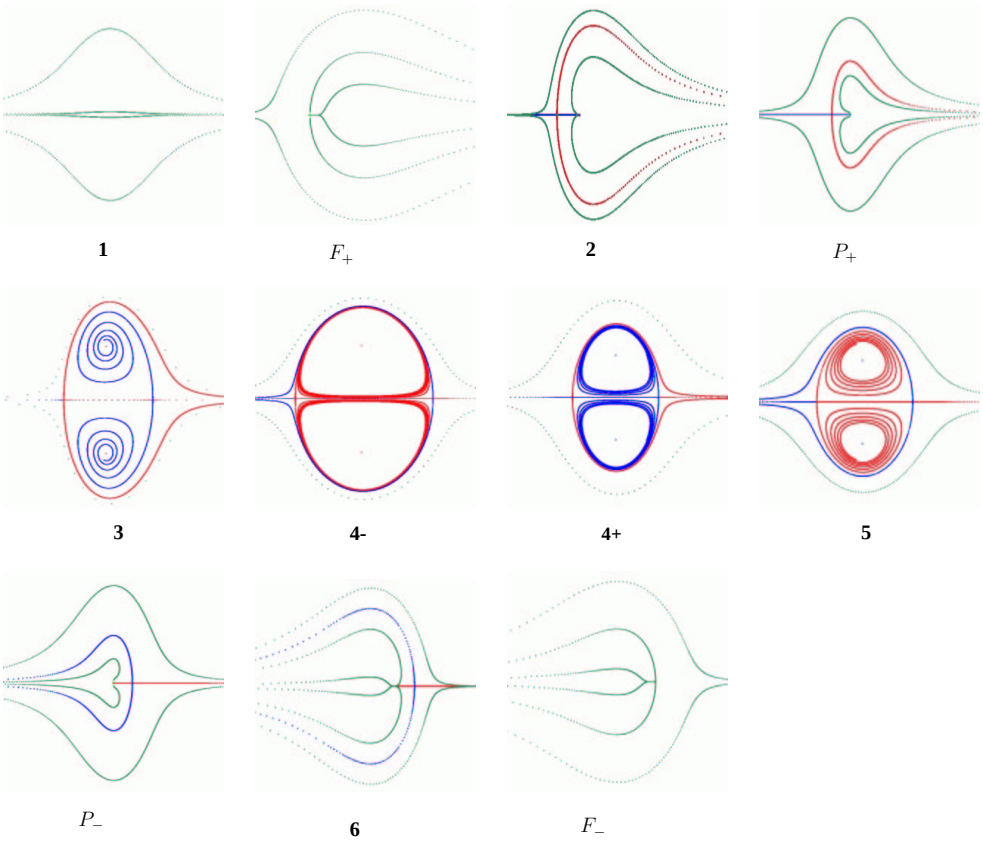

Figure 8: Map : Case 1. $a_0 > 0, b_0 > 0$

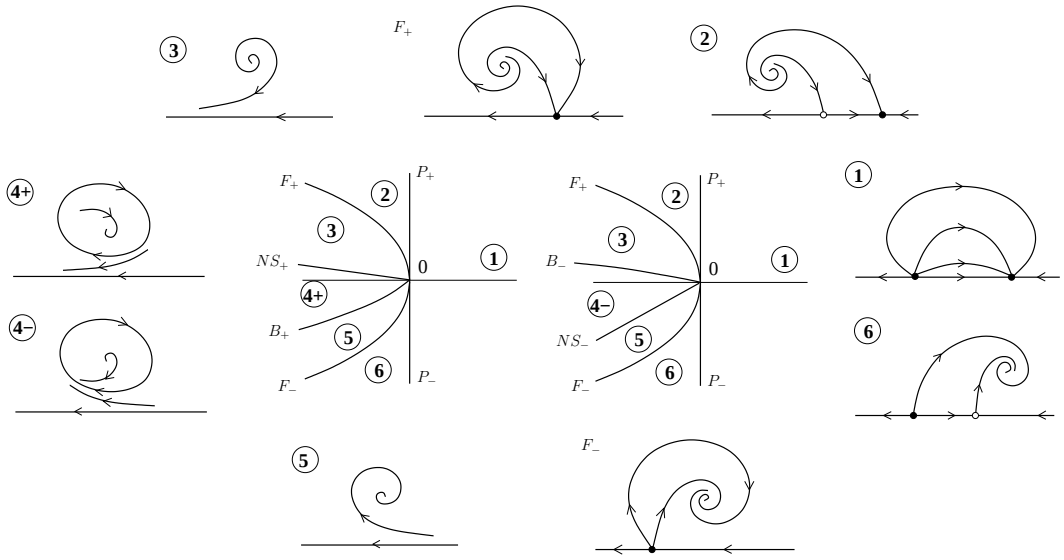

Figure 9: Vector field : Case 2. $a_0 < 0, b_0 > 0$

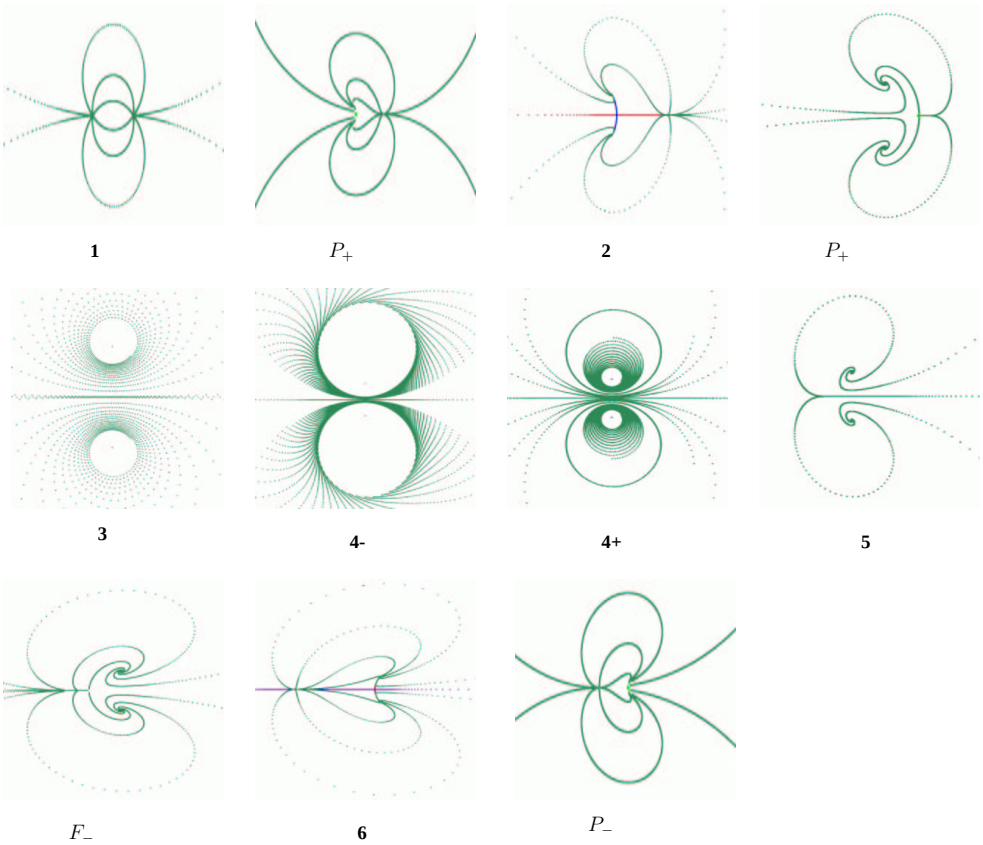

Figure 10: Map : Case 2. $a_0 < 0, b_0 > 0$

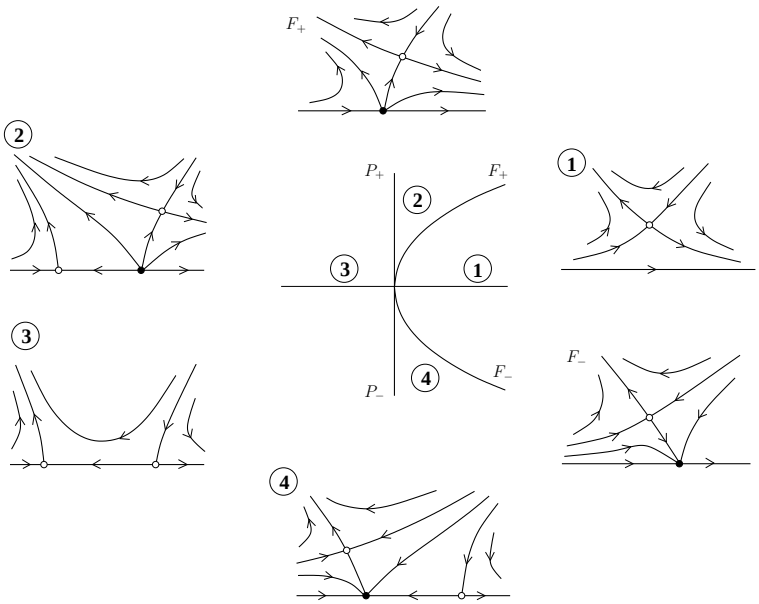

Figure 11: Vector field : Case 3. $a_0 > 0, b_0 < 0$

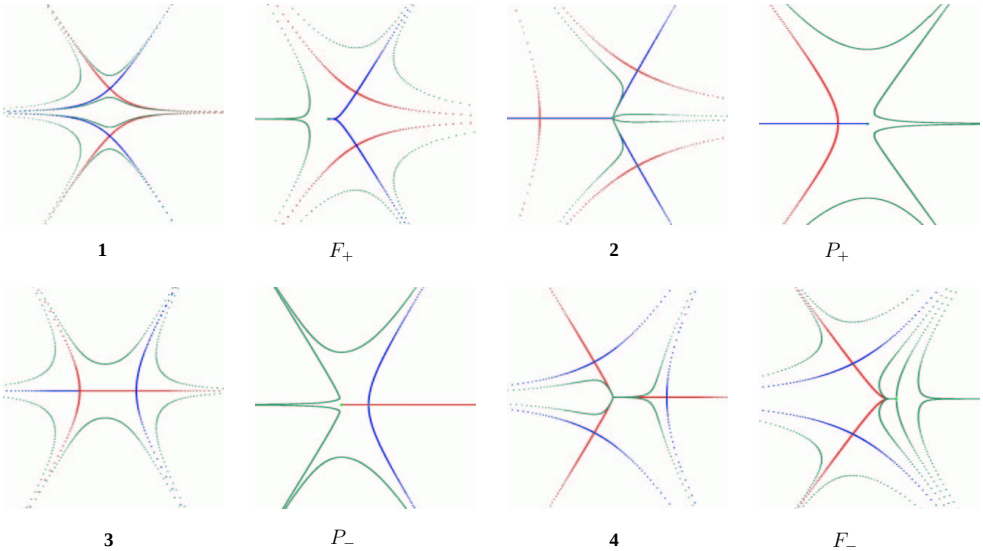

Figure 12: Map : Case 3. $a_0 > 0, b_0 < 0$

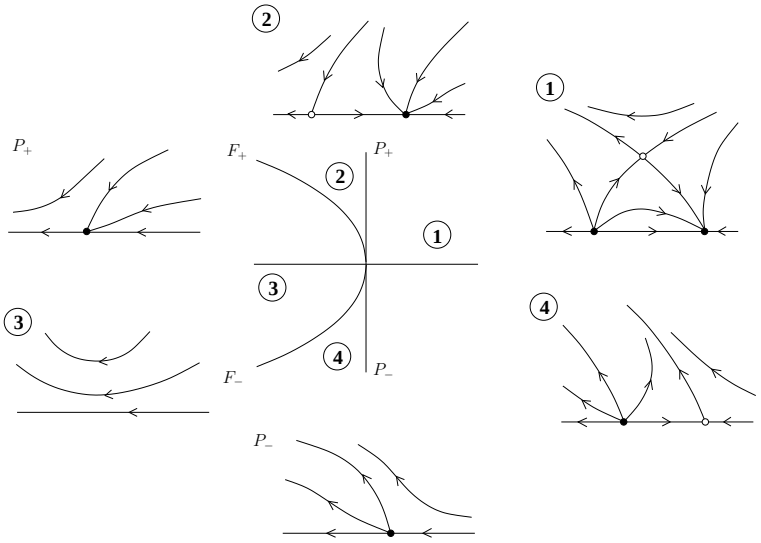

Figure 13: Vector field : Case 4. $a_0 < 0, b_0 < 0$

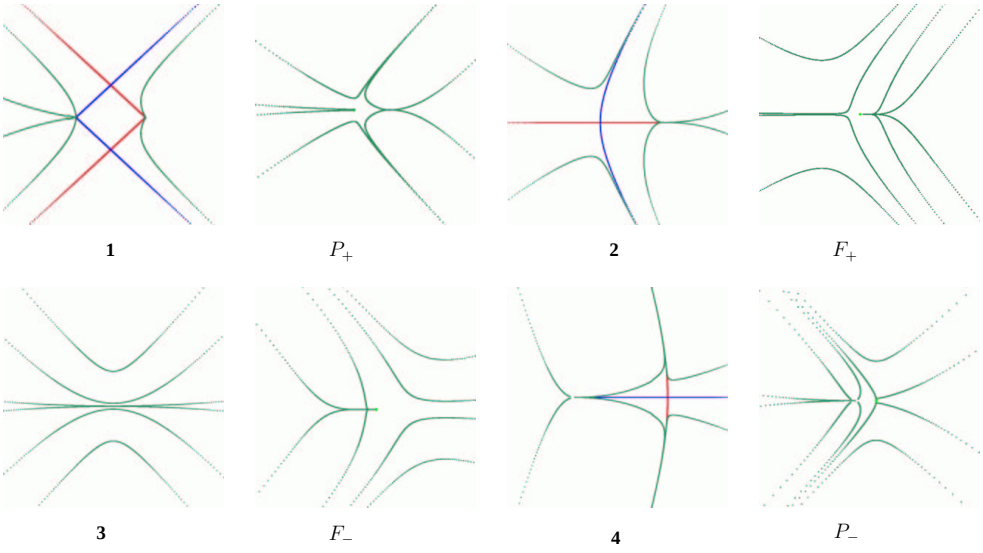

Figure 14: Map : Case 4. $a_0 < 0, b_0 < 0$

As mentioned by Gheiner [1994], there are more differences between the phase portraits of (30) and a generic (9), which are related to other heteroclinic tangencies. Indeed, in the truncated normal form (9) the x_1-axis is always invariant. Therefore, in cases 1 and 3 we have the heteroclinic connections between the saddles located on the horizontal axis. However generically, the higher order terms in (9) break the reflectional symmetry and the heteroclinic connection along the x_1-axis is lost. This allows for heteroclinic structures caused by intersections of the invariant manifolds of the saddles near the horizontal axis. These intersections can be either transversal (as in Fig. 15) or tangential. Therefore, in the first three cases, the bifurcation diagrams of (30) and a generic (9) are not locally topologically equivalent.

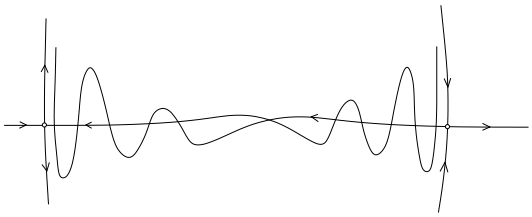

Figure 15: A transversal heteroclinic structure near the horizontal axis.

Gheiner [1994] claims that in case 3 an additional heteroclinic structure may appear: The unstable manifold of the period-2 cycle could intersect tangentially the stable manifold of a saddle fixed point on the x_1-axis. This is impossible. Indeed, if such an intersection happens, the stable manifold of the saddle on the x_1-axis must oscillate between two branches of the unstable manifold of the period-2 saddle cycle, crossing a small neighbourhood of the other fixed point on the x_1-axis which is repelling.

In case 4, Gheiner [1994] gives strong indications that (9) is locally topologically equivalent to (30), where the cubic terms can be omitted.

4 Examples

In this section we present two examples of the fold-flip bifurcation. We compute the normal form coefficients and show that the behaviour predicted by the normal form is correct.

4.1 A note on the generalized Hénon map

Consider the *generalized Hénon map*

$$\begin{pmatrix} x \\ y \end{pmatrix} \mapsto \begin{pmatrix} y \\ \alpha - \beta x - y^2 + Rxy + Sy^3 \end{pmatrix}. \tag{43}$$

Setting $R = S = 0$ one obtains the standard Hénon map. We will consider α and β as control parameters and R and S as constants. This map appears as a rescaled first return map in the study of at least two global bifurcations of maps related to codim 2 homoclinic tangencies, when:

(1) a diffeomorphism in $\mathbb{R}^2$ has a neutral saddle with a quadratic homoclinic tangency (see Gonchenko and Gonchenko [2000] and Gonchenko [2002]);

(2) a diffeomorphism in $\mathbb{R}^3$ has a saddle with a generalized homoclinic tangency (i.e., the unstable manifold of the saddle has a quadratic tangency to its stable manifold but is nontransversal to leaves of the strong stable foliation in the stable manifold at the homoclinic points) (see Gonchenko et al. [2001]).

In these studies, codim 2 local bifurcations of fixed points of (43) play an important role, since they allow to predict bifurcations of closed invariant curves. Bifurcations of (43) are well understood for $\beta > 0$, where the standard Hénon map preserves orientation. In this parameter region, strong resonance points have been found. Much less is known about bifurcations of (43) when $\beta < 0$. We show below that the map has a fold-flip point in this parameter region and compute its normal form.

For $\alpha = 0$ the map has the fixed point $(x, y) = (0, 0)$. The Jacobi matrix of (43) at this point is

$$A = \begin{pmatrix} 0 & 1 \\ -\beta & 0 \end{pmatrix}.$$

Thus, if $\beta = -1$, we have two multipliers $+1$ and -1. So we have found a fold-flip codim 2 point for all values of R and S.

First we analyse (43) without the cubic term, i.e., set $S = 0$. It is easy to verify that fixed points of this map can bifurcate at the following curves:

$$t_{fold} = \left\{(\alpha, \beta) : \alpha = \frac{(\beta+1)^2}{4(R-1)}\right\}, \quad t_{flip} = \left\{(\alpha, \beta) : \alpha = \frac{1}{4}(\beta+1)^2(3-R)\right\}.$$

Note that these two parabolas have a common point: The fold-flip point $(\alpha, \beta) = (0, -1)$. They coincide if $R = 2$, i.e., the flip bifurcation is degenerate for $R = 2$.

If we consider the second iterate of (43) with $S = 0$, a curve can be found, where a period-2 cycle has two multipliers with unit product:

$$t_{NS} = \left\{ (\alpha, \beta) \ : \alpha = \frac{(\beta+1)(\beta + R^2 - (1+R))}{R^2} \right\}.$$

To exclude neutral saddles, we should check that the multipliers are indeed complex for some values of α, β and R. Simple analysis shows that the Neimark-Sacker bifurcation occurs only if $R \neq 0$ and $R > -1$. This means that depending on whether $R < -1$ or $R > -1$ we have either the "difficult" or the "easy" case, respectively. For the difficult case we have a distinction between $R > 1$ and $R < 1$, since the fold and flip curve change position in the parameter plane when crossing $R = 1$. We sketch in Fig. 16 the bifurcation curves in the (α, β)-plane for three typical values of R. We recognize Figs. 16(a),(b) as cases 1 and 2 from Sec. 3.3, respectively,

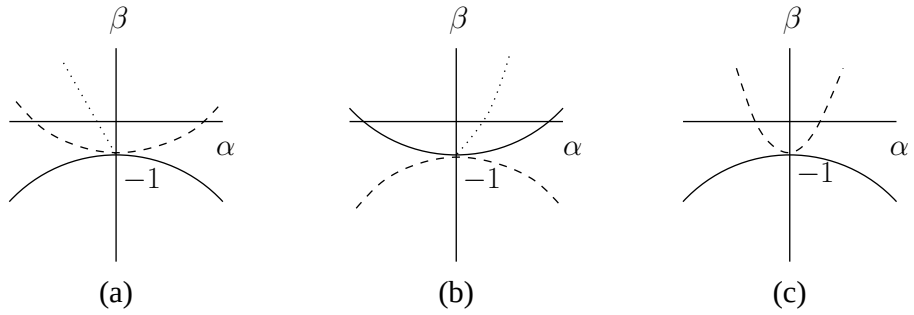

Figure 16: The (α, β)-plane: (a) case 1; (b) case 2; (c) case 3/4 . The thick/dashed line is the fold/flip curve. The dotted one is the Neimark-Sacker curve.

and Fig. 16(c) as case 3 or 4.

We now compute the critical normal form coefficients using the formulas obtained in Sec. 2.2. The eigenvectors are

$$q = 2q^* = \begin{pmatrix} 1 \\ 1 \end{pmatrix}, \ p = 2p^* = \begin{pmatrix} 1 \\ -1 \end{pmatrix},$$

while the multilinear functions are given by

$$B(x,y) = \begin{pmatrix} 0 \\ R(x_1 y_2 + x_2 y_1) - 2x_2 y_2 \end{pmatrix}, \quad C(x,y,z) = \begin{pmatrix} 0 \\ 6S x_2 y_2 z_2 \end{pmatrix}.$$

For the quadratic coefficients we find

$$a_1(0) = -(1-R), \qquad e_1(0) = -1, \qquad b_1(0) = -(R+1),$$
$$h_{2000} = \frac{1}{2}(1-R)\begin{pmatrix} 1 \\ -1 \end{pmatrix}, \quad h_{1100} = -\tfrac{1}{2}\begin{pmatrix} 1 \\ 1 \end{pmatrix}, \quad h_{0200} = \frac{1}{2}(1+R)\begin{pmatrix} 1 \\ -1 \end{pmatrix},$$

then we get

$$c_1(0) = \frac{3}{2}(1-R),\ c_2(0) = -\frac{1}{2}(1+R),\ c_3(0) = -\frac{1}{2}(1-R)^2,\ c_4(0) = \frac{3}{2}(1+R)^2.$$

The normalized coefficients of (9) are therefore

$$a(0) = (1-R),\ b(0) = (1+R),\ c(0) = \frac{3}{2}(1-R),\ d(0) = -\frac{1}{2}(5+3R)$$

(see Remark 2.2.2). We see that, indeed, depending on R the following cases occur:

	a	b	
$R < -1$	+	-	case 3
$-1 < R < 1$	+	+	case 1
$R > 1$	-	+	case 2

For cases 1 and 2 we calculate the leading term of the Lyapunov coefficient

$$c_{NS} = R^2(1-R),$$

so that the closed invariant curves appearing via the Neimark-Sacker bifurcation will be unstable in case 1 and stable in case 2.

The bifurcation structure does not change much locally, if $S \neq 0$. For $(\alpha, \beta) = (0, -1)$, we have the same critical fixed point and the same eigenvectors for the center manifold computations. The critical values for $a(0)$ and $b(0)$ remain unchanged, therefore we can distinguish the same cases 1,2 and 3, depending on R. The coefficients $c_i(0)$ are different, namely:

$$c_1(0) = \frac{3}{2}(1-R) + 3S,\ c_2(0) = -\frac{1}{2}(1+R) + 3S,$$
$$c_3(0) = -\frac{1}{2}(1-R)^2 + 3S,\ c_4(0) = \frac{3}{2}(1+R)^2 + 3S.$$

¿From these expressions we obtain the normalized critical cubic coefficients:

$$c(0) = \frac{3}{2}(1-R) + 3S,\ d(0) = -\frac{1}{2}(5+3R) + S(3+4R).$$

The Lyapunov coefficient also gets an extra term:

$$c_{NS} = R^2(1-R) + 2RS(1+2R).$$

Now, while we still have case 1 for $-1 < R < 1$, the closed invariant curve might be stable or unstable depending on a combination of R and S. Similarly, for case 2 where $R > 1$, the closed invariant curve need not be stable. We excluded $R = 0$ as exceptional. For $(\alpha, \beta, R) = (0, -1, 0)$ we actually have a codim 3 singularity, since the Lyapunov coefficient is then equal to zero.

We present in Fig. 17 some phase portraits to show the behaviour of (43) close to the fold-flip point for several values of R and S:

Subfigure	R	S	α	β
a	-2	0	.0004	-.999
b	-2	-5	.0004	-.999
c	0.5	0	.0001	-1.001
d	0.5	-2	.001	-1.001
e	3	0	.0004	-.9985
f	3	.5	.001	-.9985

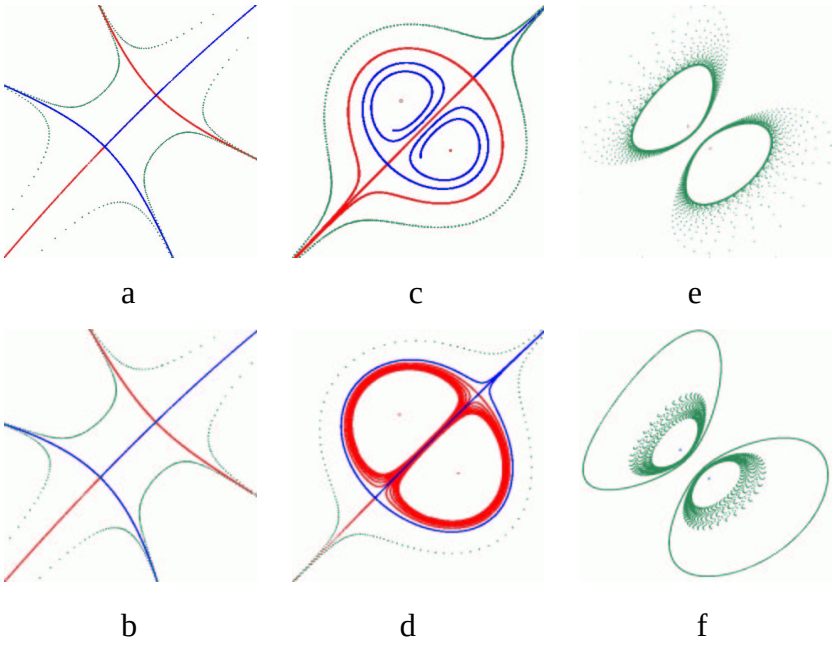

Figure 17: Selected phase portraits of (43).

4.2 The extended Lorenz Model

As an example of the fold-flip bifurcation in ODEs we study an extension of a model formulated by Lorenz [1984]. A bifurcation analysis of this model was presented by Shil'nikov et al. [1995] and van Veen [2002]. In the latter paper it was shown, that the Lorenz-84 model approximates the dynamics of a low-order Galerkin truncation of an atmospheric flow model. The atmospheric model describes synoptic dynamics, i.e., dynamics on a time scale of about a week and a length scale of about ten thousand kilometers. The synoptic atmospheric dynamics over the North Atlantic ocean is dominated by the *jet stream*, a westerly circulation, and *baroclinic waves*, which transport heat and momentum northward. In the Lorenz-84 model the intensity of the jet stream is given by X and the sine and cosine coefficients of a baroclinic wave are given by Y

$Y = -5.6335141581943.10^{-2}$	$F = 1.7620532879639$	$\lambda_1 = 1 \pm 10^{-11}$
$Z = 4.1293337647981.10^{-2}$	$T = 2.80597685.10^{-4}$	$\lambda_2 = -1 \pm 10^{-9}$
$U = .31352886978279$		$\lambda_3 = -0.43054026152942$

Table 1: The critical fixed point of the Poincaré map associated to (44) with the parameter values and the multipliers.

and Z. The dynamical equations for these variables are the first three equations in the system

$$\begin{cases} \dot{X} &= -Y^2 - Z^2 - \alpha X + \alpha F - \gamma U^2 \\ \dot{Y} &= XY - \beta XZ - Y + G \\ \dot{Z} &= \beta XY + XZ - Z \\ \dot{U} &= -\delta U + \gamma UX + T \end{cases} \tag{44}$$

The damping time scale of the baroclinic wave is about one week and is scaled to unity. As $\alpha = 1/4$ the jet stream is damped more slowly. We extend the Lorenz-84 model by adding the fourth equation in the spirit of Palmer [1995], who studied the influence on the jet stream and the baroclinic waves of external parameters such as the sea surface temperature. Note, that U interacts nonlinearly with the jet stream and that the Lyapunov function $L = X^2+Y^2+Z^2+U^2$ is conserved in the absence of linear damping and constant forcing. In the following we will fix

$$\beta = 1,\ \gamma = 0.987,\ \delta = 1.04,\ G = 0.2.$$

It is known from van Veen [2002], that the basic cycle of the Lorenz-84 model, which is created via a Hopf bifurcation of the trivial equilibrium and represents a traveling baroclinic wave, undergoes a period doubling cascade at certain values of the parameter F. By construction, solutions of the Lorenz-84 model are also solutions of the extended model for $U = T = 0$. At a period doubling bifurcation of the Lorenz-84 model a small perturbation of the extended model can yield a cycle with Floquet multipliers $+1$ and -1.

We study the Poincaré map in the plane $X = 1.05$ at the fold-flip point. In Table 1 the numerical values are listed. Figure 18 shows the bifurcation diagram obtained in a neighbourhood of the codimension 2 point. In the top left corner there is a generalized Hopf point GH at which a Hopf bifurcation and a fold bifurcation of a cycle meet (see, for example, Kuznetsov [1998], chapter 8.3). Along the fold line the cycle has one multiplier $+1$ and two multipliers within the unit circle. One of them crosses -1 at the codimension 2 fold-flip point A. From the picture and its scale we deduce that $a(0), b(0) > 0$. Secondly we expect that $a(0)$ is small, since the fold and flip curves are very close. To compute the multilinear functions, we integrated the variational equations described in Appendix A numerically using a Runge-Kutta-Felbergh scheme of 7-8 order. Then we implemented the formulas for the Poincaré map and its derivatives in MAPLE and applied the formulas of Sec. 2.2 for the center manifold reduction. This gives

$$a(0) = 0.002047,\ b(0) = 4.4010,\ c(0) = -3.2264,\ d(0) = 552.051.$$

These values are in agreement with what we deduced from Fig. 18. For these coefficients the Lyapunov coefficient has the value $c_{NS} = -15.3567$, which indicates that there is a stable

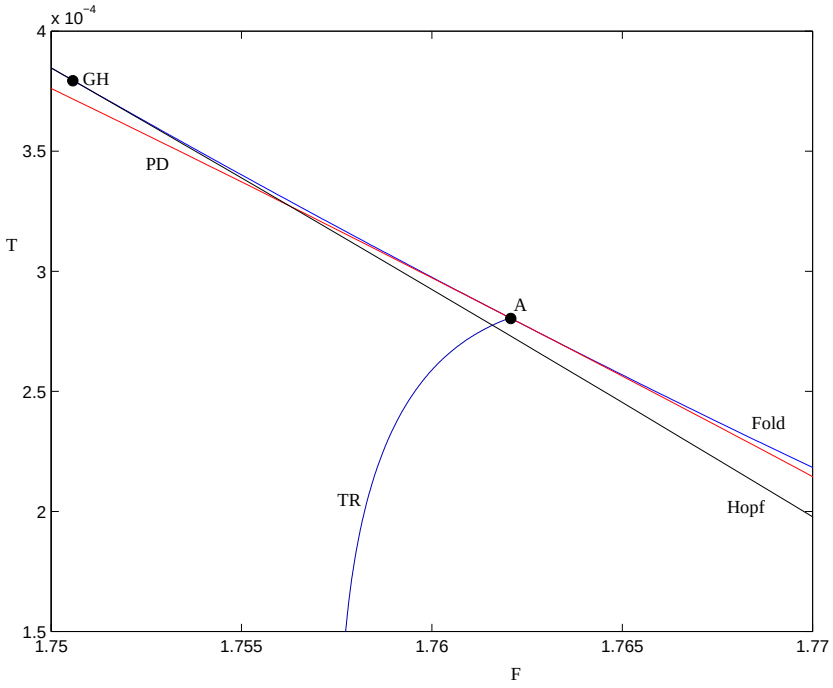

Figure 18: Bifurcation diagram near the codimension two point: Hopf (black), period-doubling (red), fold of periodic orbits (blue), torus bifurcation (darker blue). Obtained using AUTO97 Doedel et al. [1997].

invariant curve in the center manifold. A configuration of the stable invariant circles of the Poincaré map, obtained by forward integration, is shown in Fig. 19. A *double torus* around the period-2 cycle corresponds to the invariant circles of the second iterate of the Poincaré map. Also shown are the intersection points of the unstable cycle that bifurcates on the torus line TR. The period of this cycle is close to that of the motion along the stable torus. The other period of stable solutions on the torus is much longer and in fact goes to infinity at the fold-flip point A. Away from TR the torus breaks up and a strange attractor is created in a thin tube around the original invariant circle as shown in Fig. 20.

With $a(0), b(0) > 0$ we expect the torus to become heteroclinic as can be seen from the unfolding in Fig. 7. However, if we calculate the linear approximation of the heteroclinic bifurcation line J_- from proposition 3.2.2, it turns out to lie extremely close to the period doubling line PD in Fig. 18. Hence, we cannot find heteroclinic tangencies numerically. In the Poincaré section of Fig. 19, corresponding to phase portrait 4− in Fig. 8, we do see that the torus is squeezed and looks like the heteroclinic surface that exists on J_-.

Summarising, the stable solutions around the codimension 2 point A are

- an equilibrium which represents a steady jet stream without wave activity,
- period 1 and 2 cycles which represent traveling baroclinic waves, and are also present in the Lorenz-84 model itself,

- a stable torus, which represents a traveling baroclinic wave with an amplitude that is slowly modulated or
- a strange attractor, which represents a traveling baroclinic wave with an amplitude that is modulated irregularly.

The modulation of the amplitude of the traveling wave is due to interaction with the added mode, U.

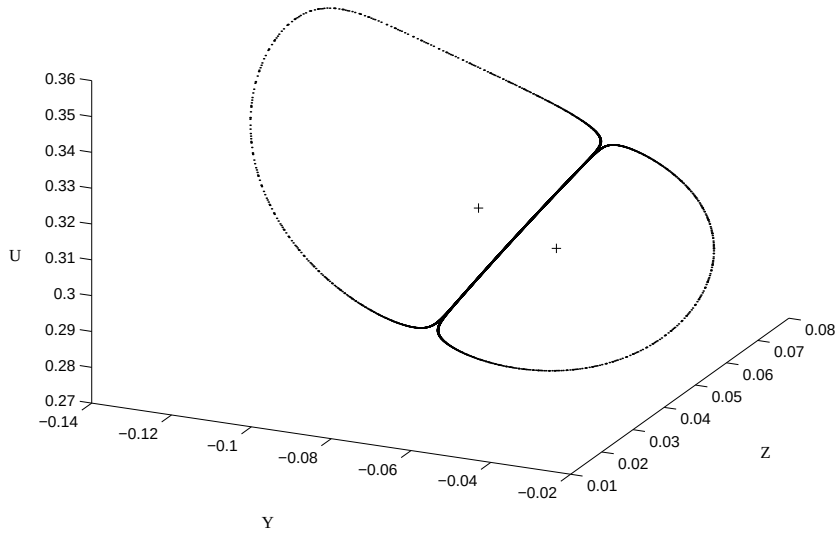

Figure 19: The invariant circles of the second iterate of the Poincaré map to the right of TR. The crosses indicate the intersection points of the unstable cycle which bifurcates on TR.

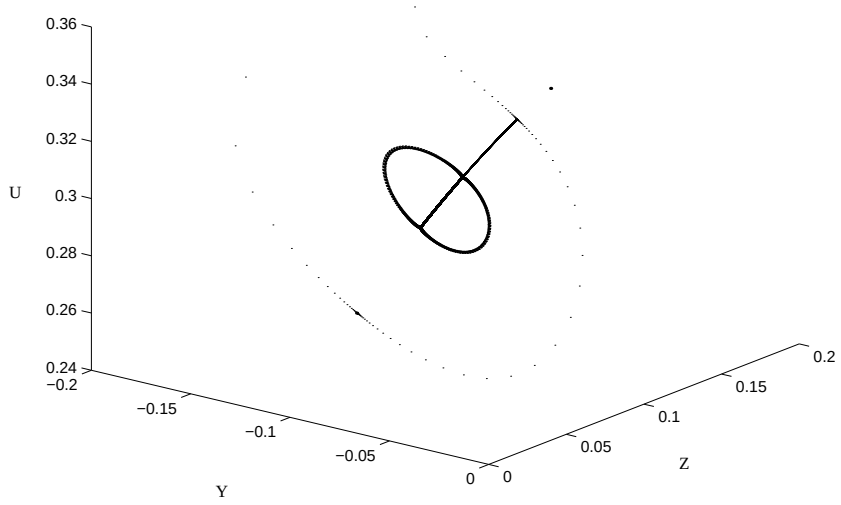

Figure 20: After the destruction of the torus a strange attractor is created. Also shown are the intersection points of the saddle type cycle. The integration was started near the saddle type orbit.

5 Discussion

In this paper we have contributed to the analysis of a codim 2 bifurcation occurring in generic two-parameter families of maps, namely the fold-flip bifurcation. We have applied our results to two examples: A generalized Hénon map and an extended Lorenz-84 ODE. Note that this bifurcation has been also found recently in another extended Lorenz-84 model by Broer et al. [2001]. In that case a periodic forcing is added and the period map is considered.

There are open numerical problems appearing while applying the theory of codim 2 bifurcations of fixed points to limit cycles in multi-dimensional ODEs. The approach based on numerical integration of the higher-order variational equations, that we have applied in Sec. 4.2, has obvious limitations. Although it works well for low-dimensional and non-stiff ODEs, a more robust approach to study codim 2 bifurcations of limit cycles has to be developed. Such an approach might combine the center manifold reduction near the cycle with a periodic normalization of the ODE on the center manifold. For first theoretical advances in this direction, see Iooss [1988] and Chow and Wang [1986].

Finally, let us note that the bifurcation behaviour of the generalized Hénon map (43) is far from being completely understood. Although the complete bifurcation diagram is likely to be never constructed, its essential global features can be analyzed using existing analytical and numerical tools. In particular, it would be interesting to investigate how the known bifurcation structures, existing for $\beta > 0$, match those emanating from the fold-flip point existing in the half-plane $\beta < 0$.

Acknowledgments

The authors are thankful to O. Diekmann and F. Verhulst (Utrecht University) for comments on an early version of the manuscript, as well as to S.V. Gonchenko (Institute for Applied Mathematics and Cybernetics, Nizhny Novgorod) for useful bibliographical remarks.

References

Arnold, V.I. [1983] *Geometrical Methods in the Theory of Ordinary Differntial Equations* (Springer-Verlag).

Arnold, V.I., Afraimovich, V.S., Il'yashenko, Yu.S. & Shil'nikov, L.P. "Bifurcation theory," In Arnold, V.I., editor, *Dynamical Systems V. Encyclopaedia of Mathematical Sciences.* (Springer-Verlag, New York), [1994] (Russian original published in 1986).

Arrowsmith, D. & Place, C. [1990] *An Introduction to Dynamical Systems* (Cambridge University Press).

Back, A., Guckenheimer, J., Myers, M.R., Wicklin, F.J. & Worfolk, P.A. [1992] "DSTools: Computer assisted exploration of dynamical systems," *Notices Amer. Math. Soc.* **39**, 303.

Beyn, W.-J., Champneys, A., Doedel, E., Govaerts, W., Kuznetsov, Yu.A. & Sandstede, B. [2002] *Handbook of Dynamical Systems, vol. 2*, chapter "Numerical Continuation, and Computation of Normal Forms", ed. Fiedler, B. (Elsevier Science, Amsterdam).

Broer, H.W., Simó, C. & Vitolo, R. [2001] "Bifurcations and strange attractors in the Lorenz-84 climate model with seasonal forcing," IWI preprint 2001-3-03, to appear in *Nonlinearity*.

Chow, S.-N., Li, C. & Wang, D. [1994] *Normal Forms and Bifurcations of Planar Vector Fields* (Cambridge University Press).

Chow, S.-N. & Wang, D. [1986] "Normal forms of bifurcating periodic orbits," *Contemp. Math.* **56**, 9–18.

Doedel, E.J., Champneys, A.R., Fairgrieve, T. F., Kuznetsov, Yu.A., Sandstede, B. & Wang, X.J. [1997] *AUTO97: Continuation and bifurcation software for ordinary differential equations (with HomCont)* Computer Science, Concordia University, Montreal, Canada.

Gavrilov, N.K. & Shil'nikov, L.P. [1972] "On three-dimensional systems close to systems with a structurally unstable homoclinic curve. part i," *Math. USSR Sb.* **17**, 467–485.

Gavrilov, N.K. & Shil'nikov, L.P. [1973] "On three-dimensional systems close to systems with a structurally unstable homoclinic curve. part ii," *Math. USSR Sb.* **19**, 139–156.

Gheiner, J. [1994] "Codimension-two reflection and nonhyperbolic invariant lines," *Nonlinearity* **7**, 109–184.

Gonchenko, S.V. & Gonchenko, V.S. [2000] "On Andronov-Hopf bifurcations of two-dimensional diffeomorphisms with homoclinic tangencies," Preprint No. 556, WIAAS, Berlin.

Gonchenko, S.V., Gonchenko, V.S. & Tatjer, J.C. "Three-dimensional dissipative diffeomorphisms with codimension two homoclinic tangencies and generalized Hénon maps," In *Proc. of Int. Conf. "Progress in Nonlinear Science" dedicated to 100th Anniversary of A.A.Andronov*, pp 63–79, [2001].

Gonchenko, S.V., Shil'nikov, L.P. & Turaev, D.V. [1996] "Dynamical phenomena in systems with structurally unstable Poincaré homoclinic orbits," *Internat. J. Bifur. Chaos* **6**, 1–17.

Gonchenko, V.S. "On bifurcations of two-dimensional diffeomorphisms with a homoclinic tangency of manifolds of a "neutral" saddle," In *Proc. Steklov Inst. Math.* **236**, pp 95–102, [2002] (in Russian).

Guckenheimer, J. & Holmes, P. [1983, 2002] *Nonlinear Oscillations, Dynamical Systems and Bifurcations of Vector Fields* (Springer-Verlag), New York.

Iooss, G. [1988] "Global characterization of the normal form for a vector field near a closed orbit," *J. Diff. Eqs.* **76**, 47–76.

Krauskopf, B. & Osinga, H. [1998]a "Globalizing two-dimensional unstable manifolds of maps," *Internat. J. Bifur. Chaos* **8**, 483–503.

Krauskopf, B. & Osinga, H. [1998]b "Growing 1D and quasi-2D unstable manifolds of maps," *J. Comp. Physics* **146**, 404–419.

Kuznetsov, Yu.A. [1998] *Elements of Applied Bifurcation Theory, 2nd edition* (Springer, New York).

Kuznetsov, Yu.A. [1999] "Numerical normalization techniques for all codim 2 bifurcations of equilibria in ODE's," *SIAM J. Numer. Anal.* **36**, 1104–1124.

Lorenz, E.N. [1984] "Irregularity: a fundamental property of the atmosphere," *Tellus* **36A**, 98–110.

Palmer, T.N. [1995] "The influence of north-west Atlantic sea surface temperature: An unplanned experiment," *Weather* **30**, 413–419.

Shil'nikov, A.L., Nicolis, G. & Nicolis, C. [1995] "Bifurcation and predictability analysis of a low-order atmospheric circulation model," *Internat. J. Bifur. Chaos* **5(6)**, 1701–1711.

Simó, C. [1989] *Modern Methods in Celestial Mechanics, Proceedings of the 13th spring school on astrophysics in Goutelas*, chapter "On the analytical and numerical approximation of invariant manifolds", eds. Benest, D. and Froeschlé, C. (Edition Frontières, Gift-sur Yvette, France).

Takens, F. [1974] "Forced oscillations and bifurcations," *Comm. Math. Inst. Rijksuniversiteit Utrecht* **3**, 1–59 (reprinted in "Global Analisys of Dynamical Systems", Broer H. *et al.* (eds.), Institute of Pysiscs Publishing, Bristol and Philadelphia, 2001).

Veen, L.van [2002] "Baroclinic flow and the Lorenz-84 model," *Internat. J. Bifur. Chaos.* to appear.

A Poincaré Maps and Their Derivatives

In this appendix we derive a method to compute numerically the derivatives of a Poincaré map up to and including third order. Let $f(x)$ be a smooth vector field in $\mathbb{R}^n$. We take a *local cross-section* $\Sigma \subset \mathbb{R}^n$ with dimension $n-1$. The hypersurface Σ does not need to be a coordinate plane, but should be chosen transversal to the flow of f. This is satisfied if for the normal $n_\Sigma(x)$ for $x \in \Sigma$ we have $\langle f(x), n_\Sigma(x)\rangle \neq 0$. Let L_0 be a τ_0-periodic orbit through Σ and $U \subset \Sigma$ a subset which contains an intersection point x_0 of $L_0 \cap \Sigma$. If L_0 intersects Σ in multiple points we shrink U until we have one point of intersection, i.e., x_0. The *Poincaré map* $P : U \to \Sigma$ is defined for $x \in U$ by

$$P(x) = \phi(t(x), x),$$

where $t(x)$ is the arrival time after which the orbit intersects Σ for the first time again, and $\phi(t, x)$ is the solution to

$$\dot{x} = f(x),\ x \in \mathbb{R}^n,$$

with the initial condition $\phi(0, x) = x$ (see Fig. 21). Note that ϕ is as smooth as f. The arrival time τ depends on x but $t(x_0) = \tau_0$. The Floquet multipliers of L_0 can be calculated as the eigenvalues of the monodromy matrix $\frac{\partial\phi(\tau_0,x)}{\partial x}$. This matrix always has a trivial eigenvalue 1. With the Liouville Theorem one can prove that the product of the multipliers is always positive.

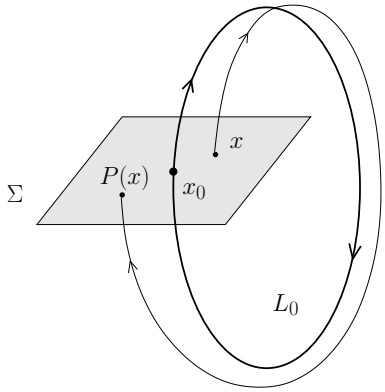

Figure 21: The geometry of the Poincaré map

We proceed with a method to derive the Poincaré map and its derivatives numerically. We closely follow the presentation of Simó [1989], but we extend it to the third order derivatives. We can write for a displacement $x + h \in \mathbb{R}^n$

$$\phi(t, x+h) = \phi(t, x) + \frac{\partial\phi(t,x)}{\partial x}h + \frac{1}{2}\frac{\partial^2\phi(t,x)}{\partial x^2}h^2 + \ldots$$

We assume that $(x + h) \in \Sigma$, or, more precisely, $\frac{\partial\phi(t,x)}{\partial x}h = (D_x\phi(t, x))(h)$, $\frac{\partial^2\phi(t,x)}{\partial x^2}h^2 = (D_x^2\phi(t, x))(h, h)$ etcetera. The multilinear functions $\frac{\partial^i\phi(t,x)}{\partial x^i}$ satisfy the variational equations,

which we find by successive differentiation of $\dot{\phi}(t,x) = f(\phi(t,x))$. Since f and ϕ are $\mathcal{C}^r$ we can change the order of the derivatives and find

$$\begin{aligned}
\frac{d}{dt}\frac{\partial\phi(t,x)}{\partial x} =& Df(\phi(t,x))\frac{\partial\phi(t,x)}{\partial x},\\
\frac{d}{dt}\frac{\partial^2\phi(t,x)}{\partial x^2} =& D^2f(\phi(t,x))\left(\frac{\partial\phi(t,x)}{\partial x}\right)^2 + Df(\phi(t,x))\frac{\partial^2\phi(t,x)}{\partial x^2},\\
\frac{d}{dt}\frac{\partial^3\phi(t,x)}{\partial x^3} =& D^3f(\phi(t,x))\left(\frac{\partial\phi(t,x)}{\partial x}\right)^3 + 3D^2f(\phi(t,x))\left(\frac{\partial^2\phi(t,x)}{\partial x^2}, \frac{\partial\phi(t,x)}{\partial x}\right) + Df(\phi(t,x))\frac{\partial^3\phi(t,x)}{\partial x^3}.
\end{aligned}$$

The initial conditions are given by

$$\left.\frac{\partial\phi(t,x)}{\partial x}\right|_{t=0} = I_n, \qquad \left.\frac{\partial^2\phi(t,x)}{\partial x^2}\right|_{t=0} = 0, \qquad \text{and } \left.\frac{\partial^3\phi(t,x)}{\partial x^3}\right|_{t=0} = 0.$$

An analytic solution to the variational equations can only be obtained in exceptional cases, but numerically we can integrate these equations and we will show how to use them to compute the derivatives of the Poincaré map. Normally one considers a cross-section Σ and the Poincaré map is just the return map to Σ. This is the case when one looks at periodic orbits, which account for fixed points of the Poincaré map. However, we will set up the structure of the Poincaré map for a flow from a cross-section Σ_1 to a cross-section Σ_2 to distinguish between the initial and the final cross-section. In this way the notation is clearer, but in the end we will set $\Sigma_1 = \Sigma_2$. The sections are defined by equations $g_1(x) = 0$ and $g_2(x) = 0$ respectively and we assume both sections to be transversal to the flow.

Let $x_1 \in \Sigma_1$ be the initial point and define $P : \Sigma_1 \to \Sigma_2$ by $P(x_1) = x_2 = \phi(t(x_1, x_1))$, such that $g_2\big(\phi(t(x_1), x_1)\big) = 0$. Here $t(x_1)$ is the travel time and it depends, of course, on the initial point. We compute the first derivative of P by differentiation with respect to x_1

$$\frac{\partial P}{\partial x_1} = f(x_2)\frac{\partial t}{\partial x_1} + \frac{\partial\phi}{\partial x_1}\big(t(x_1), x_1\big). \tag{45}$$

Remark A.0.1 We add a word of caution. We should make a distinction between the variables of the ODE in $\mathbb{R}^n$ and the variables of the Poincaré map in $\Sigma \sim \mathbb{R}^{n-1}$. The derivatives above are formal w.r.t. $x_1 \in \mathbb{R}^n$, but the LHS of (45) has the domain Σ_1. Therefore the RHS has to be restricted to Σ_1. Now, if we take $\Sigma_1 = \Sigma_2$ to be given by setting the n-th coordinate equal to a constant, then the derivatives of the Poincaré map will contain a block of zeros, namely for the n-th component. This result follows easily from (46) and (49) for the linear and quadratic part and can be extended for higher orders. In this way we can take the variables $\{x_1, \ldots, x_n\}$ of f in $\mathbb{R}^n$ as variables for the Poincaré map, excluding the n-th.

The first variational equation provides the matrix $\frac{\partial\phi}{\partial x_1}$. The derivative $\frac{\partial t}{\partial x_1}$ is still unknown. We obtain it by differentiating the relation $g_2\big(\phi(t(x_1), x_1)\big) = 0$

$$\langle Dg_2(x_2), \left(f(x_2)\frac{\partial t}{\partial x_1} + \frac{\partial\phi}{\partial x_1}\big(t(x_1), x_1\big)\right)\rangle = 0,$$

or

$$\frac{\partial t}{\partial x_1} = -\frac{1}{\langle \nabla g_2(x_2), f(x_2)\rangle} Dg_2 \frac{\partial \phi}{\partial x_1}.$$

Note that the transversality condition implies that the denominator is nonzero. Now we suppose that Σ_1 and Σ_2 are just coordinate planes, i.e., g_1 and g_2 are given by taking, for instance the last coordinate equal to a constant. We write $a_{ij} = \frac{\partial \phi_i}{\partial x_{1,j}}\big(t(x_1), x_1\big)$. Then we have $\frac{\partial t}{\partial x_{1,i}} = -\frac{a_{ni}}{f_n(x_2)}$ and the elements of the $(n-1)\times(n-1)$ matrix $\frac{\partial P}{\partial x_1}(x_1)$ are given by

$$\Big(\frac{\partial P}{\partial x_1}\Big)_{ij} = a_{ij} - \frac{f_i(x_2)}{f_n(x_2)} a_{nj}. \tag{46}$$

The restriction to the first $n-1$ components is given by taking $1 \le i, j \le n-1$.

We continue with the second derivative. We differentiate another time and we find

$$\frac{\partial^2 P}{\partial x_1^2} = Df(x_2)f(x_2)\Big(\frac{\partial t}{\partial x_1}\Big)^2 + 2Df(x_2)\frac{\partial \phi}{\partial x_1}\frac{\partial t}{\partial x_1} + f(x_2)\frac{\partial^2 t}{\partial x_1^2} + \frac{\partial^2 \phi}{\partial x_1^2}.$$

Note that the first variational equation is used here to simplify the derivatives. As before $\frac{\partial^2 \phi}{\partial x_1^2}$ is obtained from the second variational equation and $\frac{\partial^2 t}{\partial x_1^2}$ by differentiating $g\big(\phi(t(x_1), x_1)\big)$ once more

$$D^2 g_2(x_2))\Big(f(x_2)\frac{\partial t}{\partial x_1} + \frac{\partial \phi}{\partial x_1}\Big)^2 + Dg_2(x_2)\Big[Df(x_2)f(x_2)\Big(\frac{\partial t}{\partial x_1}\Big)^2 \tag{47}$$

$$+2Df(x_2)\frac{\partial \phi}{\partial x_1}\frac{\partial t}{\partial x_1} + f(x_2)\frac{\partial^2 t}{\partial x_1^2} + \frac{\partial^2 \phi}{\partial x_1^2}\Big] = 0, \tag{48}$$

or more compactly (using (45) and (47))

$$D^2 g_2(x_2)\Big(\frac{\partial P}{\partial x_1}\Big)^2 + Dg_2(x_2)\frac{\partial^2 P}{\partial x_1^2} = 0.$$

For notational clarity we drop from now on the subscript $_1$ in x_1. All derivatives are now with respect to (the components x_j of) x or to t. Returning to the specific case of a return map we introduce the notation $b_{ijk} = \frac{\partial^2 \phi_i}{\partial x_j \partial x_k}$, $f_i = f_i(x_2)$ and $f_{ij} = D_i f_j(x_2)$. Making these substitutions also for the time derivatives, we obtain

$$\frac{\partial^2 P_i}{\partial x_j \partial x_k} = b_{ijk} - \frac{f_i}{f_n} b_{njk} + \frac{1}{f_n}\sum_{s=1}^{n}\Big(f_{si} - \frac{f_i}{f_n} f_{sn}\Big)\Big(\frac{f_s}{f_n} a_{nj} a_{nk} - a_{sk} a_{nj} - a_{sj} a_{nk}\Big). \tag{49}$$

As before we have $1 \le i, j, k \le n-1$.

Finally we calculate the third derivative as well. Differentiating one more time, we find

$$\begin{aligned}\frac{\partial^3 P}{\partial x^3} &= D^2 f(x_2)\Big(f^2(x_2)\Big(\tfrac{\partial t}{\partial x}\Big)^3 + 3f(x_2)\tfrac{\partial \phi}{\partial x}\Big(\tfrac{\partial t}{\partial x}\Big)^2 + 3\Big(\tfrac{\partial \phi}{\partial x}\Big)^2\tfrac{\partial t}{\partial x}\Big)\\ &+Df(x_2)^2\Big(f(x_2)\Big(\tfrac{\partial t}{\partial x}\Big)^3 + 3\tfrac{\partial \phi}{\partial x}\Big(\tfrac{\partial t}{\partial x}\Big)^2\Big) + f(x_2)\tfrac{\partial^3 t}{\partial x^3} + \tfrac{\partial^3 \phi}{\partial x^3}\\ &+3Df(x_2)\Big(f(x_2)\tfrac{\partial t}{\partial x}\tfrac{\partial^2 t}{\partial x^2} + \tfrac{\partial \phi}{\partial x}\tfrac{\partial^2 t}{\partial x^2} + \tfrac{\partial \phi}{\partial x^2}\tfrac{\partial t}{\partial x}\Big).\end{aligned}$$

More explicitly in coordinates we have

$$\begin{aligned}\frac{\partial^3 P_i}{\partial x_j \partial x_k \partial x_l} &= \sum_{r,s=1}^{n} D_{rs} f_i(x_2) \left(f_r f_s \frac{\partial t}{\partial x_j}\frac{\partial t}{\partial x_k}\frac{\partial t}{\partial x_l} + f_s \frac{\partial \phi_r}{\partial x_j}\frac{\partial t}{\partial x_k}\frac{\partial t}{\partial x_l}^{*} + \frac{\partial \phi_r}{\partial x_j}\frac{\partial \phi_s}{\partial x_k}\frac{\partial t}{\partial x_l}^{*} \right) \\ &+ \sum_{r,s=1}^{n} D_s f_i(x_2) D_r f_s(x_2) \left(f_r \frac{\partial t}{\partial x_j}\frac{\partial t}{\partial x_k}\frac{\partial t}{\partial x_l} + \frac{\partial \phi_r}{\partial x_j}\frac{\partial t}{\partial x_k}\frac{\partial t}{\partial x_l}^{*} \right) \\ &+ \sum_{s=1}^{n} D_s f_i(x_2) \left(f_s(x_2) \frac{\partial t}{\partial x_j}\frac{\partial^2 t}{\partial x_k \partial x_l}^{*} + \frac{\partial \phi_s}{\partial x_j}\frac{\partial^2 t}{\partial x_k \partial x_l}^{*} + \frac{\partial^2 \phi_s}{\partial x_j \partial x_k}\frac{\partial t}{\partial x_l}^{*} \right) \\ &+ f_i \frac{\partial^3 t}{\partial x_j \partial x_k \partial x_l} + \frac{\partial^3 \phi_i}{\partial x_j \partial x_k \partial x_l}.\end{aligned} \tag{50}$$

Here the $*$ means that the term with j,k,l cyclically permuted should be included as well. The above expression is then invariant under changing the order of the differentiation, if f is smooth. The third order derivative of the time can be found from

$$D^3 g_2(x_2) \left(\frac{\partial P}{\partial x} \right)^3 + 3 D g_2^2(x_2) \frac{\partial^2 P}{\partial x^2}\frac{\partial P}{\partial x} + D g_2(x_2) \frac{\partial^3 P}{\partial x^3} = 0.$$